



**HAL**  
open science

## **A minimum set of stable blocks for rational design of polypeptide chains Running head: A set of stable blocks for protein rational design**

Alexei N Nekrasov, Ludmila G Alekseeva, Rudolf A. Pogosyan, Dmitry A Dolgikh, M.P. P Kirpichnikov, Alexandre de Brevern, Anastasia A Anashkina

### ► To cite this version:

Alexei N Nekrasov, Ludmila G Alekseeva, Rudolf A. Pogosyan, Dmitry A Dolgikh, M.P. P Kirpichnikov, et al.. A minimum set of stable blocks for rational design of polypeptide chains Running head: A set of stable blocks for protein rational design. *Biochimie*, 2019, 160, pp.88-92. <10.1016/j.biochi.2019.02.006>. <inserm-02266188>

**HAL Id: inserm-02266188**

**<https://inserm.hal.science/inserm-02266188v1>**

Submitted on 13 Aug 2019

HAL is a multi-disciplinary open access archive for the deposit and dissemination of scientific research documents, whether they are published or not. The documents may come from teaching and research institutions in France or abroad, or from public or private research centers.

L'archive ouverte pluridisciplinaire HAL, est destinée au dépôt et à la diffusion de documents scientifiques de niveau recherche, publiés ou non, émanant des établissements d'enseignement et de recherche français ou étrangers, des laboratoires publics ou privés.



HAL Authorization

## **A minimum set of stable blocks for rational design of polypeptide chains**

Running head: **A set of stable blocks for protein rational design**

Alexei N. Nekrasov<sup>1</sup>, Ludmila G. Alekseeva<sup>1</sup>, Rudolf A. Pogosyan<sup>1</sup>, Dmitry A. Dolgikh<sup>1</sup>,  
M.P. Kirpichnikov<sup>1</sup>, Alexandre G. de Brevern<sup>2\*</sup>, Anastasia A. Anashkina<sup>3</sup>

<sup>1</sup> Shemyakin-Ovchinnikov Institute of Bioorganic Chemistry, The Russian Academy of Sciences, Miklukho-Maklaya St. 16/10, 117997, Moscow, Russia

<sup>2</sup> INSERM UMR S-1134, DSIMB, Univ. Paris Diderot, Sorbonne Paris Cite, Univ de la Reunion, Univ des Antilles, INTS, lab. of excellence GR-Ex 6, rue Alexandre Cabanel 75739 Paris Cedex 15, France

<sup>3</sup> Engelhardt Institute of Molecular Biology, Russian Academy of Sciences, Vavilov St. 32, 119991 Moscow, Russia

**Contacts:** [alexandre.debrevern@univ-paris-diderot.fr](mailto:alexandre.debrevern@univ-paris-diderot.fr), [nastya@eimb.ru](mailto:nastya@eimb.ru)

**Supplementary Information.** Supplement.doc

### **Abstract**

The aim of this work was to find a minimal set of structurally stable pentapeptides, which allows forming a polypeptide chain of a required 3D structure. To search for factors that ensure structural stability of the pentapeptide, we generated peptide sequences with no more than three functional groups, based on the alanine pentapeptide AAAAA. We analyzed 44,860 structures of peptides by the molecular dynamics method and found that 1,225 pentapeptides over 80% of the simulation time were in a stable conformation. Clustering of these conformations revealed 54 topological types of conformationally stable pentapeptides. These conformations relate to different combined elements of the protein secondary structure. So, we obtained a minimal set of amino acid structures of conformationally stable pentapeptides, creating a complete set of different topologies that ensure the formation of pre-folded conformation of protein structures.

## 1. Introduction

The folding of short peptide fragments is seldom discussed as they normally adopt random-coil conformations in water. It is believed that interacting with proteins, peptides take a certain conformation. Different authors underlined that both individual peptides in solution and peptides within proteins can have conformational preferences. They can be detected experimentally by examining peptides in solution, analyzing the structure of proteins, and conducting molecular dynamics in silico. Hatakeyama and co-workers have studied the latent propensity of short peptides to adopt folded conformations, alanine-rich peptides were placed in the cavity of self-assembled host. They found that these peptide fragments adopted specific conformations within the protected cavity [1]. Study of PDB-files demonstrated that of the 160,000 combinatorially possible tetrapeptides 1,500 adopted conformations similar to protein structures [2]. By analyzing 133 8-residue fragments from six different proteins by molecular dynamics, it was found that 85 peptides do not have a preferred structure, and 48 of them converge to the preferred structure [3].

Analyzing the structure of proteins from the Protein DataBank (<https://www.rcsb.org/>), de Brevern et al. proposed a structural alphabet of small 3D structural prototypes called Protein Blocks (PBs) [4]. This structural alphabet includes 16 PBs, each one is defined by the ( $\phi$ ,  $\psi$ ) dihedral angles of 5 consecutive residues [5]. The size of Protein Blocks corresponds to the maximum length of fragments preserving a minimum of informational entropy [6].

Three-dimensional protein structures can be described with a library of 3D fragments that define a structural alphabet. Etchebest et al. have shown that the geometrical features of the different PBs are preserved (local RMSD value equal to 0.41 Å on average) and sequence-structure specificities reinforced when databanks are enlarged [7]. PBs are short motifs capable of representing most of the local structural features of a protein backbone. Alignment of these local features as sequence of symbols enables fast detection of structural similarities between two proteins [8]. PB-based pairwise structural alignment method based on dynamic programming with a dedicated PB Substitution Matrix (SM) gave an excellent performance, when compared to other established methods for mining [9]. Based on PB, multiple structural alignment method

realized in a web server called multiple Protein Block Alignment (mulPBA) [10]. Using the algorithm based on protein blocks, a database of structural alignments (DoSA) was created. DoSA provides unique information about 159,780 conformationally similar and 56,140 conformationally dissimilar Structurally Variability Regions in 74,705 pairwise structural alignments of homologous proteins [11]. PB description of local structures was used to analyze conformations that are preferred sites for structural variations and insertions, among group of related folds [12]. Local structure prediction tool PB-kPRED based on representation of structure of a protein as a string of Protein Blocks and using the structural information from homologues in preference, if available. The method achieved mean accuracies ranging from 40.8% to 66.3% depending on the availability of homologues [13].

Also the structural alphabet was used to predict the loops connecting two repetitive structures [14]. Furthermore, it has been shown that protein structure can be described by a limited set of recurring local structures. In this context, a library composed of 120 overlapping long structural prototypes (LSPs) representing fragments of 11 residues in length and covering all known local protein structures was established [15]. On the basis of LSPs, a novel prediction method that proposes structural candidates in terms of LSPs along a given sequence was developed. This methodology was used to predict protein flexibility [15]. Then three flexibility classes were defined and proposed a method based on the LSP prediction method for predicting flexibility along the sequence. The method is implemented in PredyFlexy web server [16].

In this paper we focus on a minimal set of structurally stable pentapeptides for rational design of polypeptide chain with desirable three-dimensional structure. The pentapeptides were tested using molecular dynamics simulations. Structurally stable pentapeptides are peptides, which were in the same conformation state more than 80% of the simulation time. To search for factors that ensure structural stability of the pentapeptide, we selected peptide sequences with no more than three functional groups, based on the alanine pentapeptide AAAAA.

## 2. Methods

### 2.1 Pentapeptide sequence dataset

There are  $20^5=3\ 200\ 000$  possible pentapeptide sequences of 20 types of amino acid residues. Study of stability for this number of pentapeptides by molecular dynamics method is very time consuming. We assumed that the three functional groups should be sufficient to form a stable conformational state of the pentapeptide. We wanted to study the effect of the amino acid residue positions on its stability. So we proposed the following scheme for the generation of pentapeptide sequences.

The alanine pentapeptide was taken as a matrix, since glycines in the polypeptide chain possess additional conformational space due to the absence of a side radical. Three residues of this alanine pentapeptide — one in the central position (position “0”) and two more in other positions (positions -2, -1, +1, and +2) were sequentially replaced by all possible amino acid residues of 20 canonical amino acids. The number of possible pairs of two replaced amino acids positions in the pentapeptide is 6 (substitutions at -2 and -1, -1 and 1, -2 and 2, -1 and 1, -1 and 2, 1 and 2 positions are possible), therefore the number of possible combinations is  $20^3 * 6 = 48000$ . However, in this approach  $20 * (20 * 6 + 6 * 6 + 1)$  identities are formed, associated with the presence of an alanine matrix. Thus, subtracting the identities, we get 44860 possible unique sequences. It can be seen that there is a strong overrepresentation of alanines at positions -2, -1, +1, +2. All residues except alanine are found at these positions 1160 times each and alanine is found 22820 times. At position 0 all amino acid residues are found 2243 times each.

Due to this scheme for pentapeptide sequence generation one can evaluate the contribution of each position to the pentapeptide stability and the influence of the amino acid type in a particular position on the stability of the pentapeptide.

### 2.2 Molecular modeling of the pentapeptide structure by molecular dynamics method

C-terminus of each pentapeptide was protected by methyl group and N-terminus was protected by acetyl group. These caps have removed the effect of the end charges of the polypeptide chain on the conformational states obtained in MD modeling.

Force field AMBER/OPLS was used [17,18] for molecular dynamics simulation performed with X-PLOR (Version 3.1) software

(<http://www.csb.yale.edu/userguides/datamanip/xplor/xplorman/node1.html>) with personal license from Axel T. Brünger. The starting conformation of all pentapeptides was unfolded (extended) ( $\phi=180.0^\circ$ ;  $\psi=180.0^\circ$ ). Molecular modeling of pentapeptides started from extended conformation within 10,000 picoseconds at 300K with 0.001 picosecond integration step. We saved 5,000 current conformational states for each pentapeptide after 5,000 picoseconds of relaxation process, one state per picosecond. This AMBER/OPLS force field was chosen because the original peptide conformation is unfolded. CHARMM force fields work well near local minima, but in the case of three-dimensional hindrances they lead to unpredictable results. We did not use a solvent in the molecular dynamics experiment. Solvent is important for polypeptide chains capable of forming a “hydrophobic core”. Pentapeptides are too short to possess this ability. This approach was approved by many years of conformational analysis of short peptides [19,20]. The complete molecular dynamics protocol is provided in the Supplement.

### *2.3 Clustering of pentapeptide conformational states*

Molecular dynamics trajectory with 5,000 conformational states was subjected to clustering analysis to split it into a few clusters of the structurally similar conformations. The squared Euclidean distance of torsion angles phi and psi of polypeptide backbone (a total of 8 angles for each pentapeptide) was chosen as distance measure between conformational states of molecular dynamics trajectory. Clustering was carried out by unweighted pair-group method using the centroid average [21] (program “condense”, <https://fap.sbras.ru>). A clustering threshold of 0.15 was used.

Figure 1 shows the size of the two largest clusters of conformational states of molecular-dynamic trajectories for 44,860 pentapeptides. There is a local maximum of the distribution in the lower right corner. It corresponds to the size of the largest cluster of more than 4,000 states, i.e. 80% of the conformational states under consideration. So, the threshold of 80% of the conformational states was chosen for the criterion of structural stability. Pentapeptides where more then 80% of all conformational states were within the same cluster, were called "structurally stable elements" or "structurally stable pentapeptides". The structure closest to the cluster center was selected as the cluster

representative. Each structurally stable pentapeptide was characterized by the representative.

#### *2.4 Clustering of different structurally stable pentapeptides*

To identify common topological types among the obtained structurally stable pentapeptides, representative structures were subjected to the same clustering procedure described above. As a result, 54 clusters of structurally stable structural elements with different topologies were obtained (Supplement, Table 1). Each of 54 cluster of structurally stable pentapeptide was characterized by the structure closest to the cluster center (Supplement, Table 2).

#### *2.5 Comparison of idealized secondary structures with spatial structures of model pentapeptides*

To identify the functional role that structurally stable pentapeptides can play in the protein structure, a comparison of the Cartesian coordinates of the  $C\alpha$  atoms of three consecutive amino acid residues of the pentapeptide located at the N- and C-termini of the pentapeptides with idealized secondary structures was performed:  $\alpha$ -helix ( $\varphi=-57.0^\circ$ ;  $\psi=-47.0^\circ$ ), anti-parallel  $\beta$ -structure ( $\varphi=-139.0^\circ$ ;  $\psi=+135.0^\circ$ ) and parallel  $\beta$ -structure ( $\varphi=-119.0^\circ$ ;  $\psi=+113.0^\circ$ ) [22]. To combine spatial structures, the MaxCluster program was used (<http://www.sbg.bio.ic.ac.uk/maxcluster/>).

### **3. Results**

We supposed that stability could be provided by the interaction of two or three functional groups within the pentapeptide. So, it is no need to consider all 3,200,000 possible sequences of pentapeptides to study the factors of high structural stability of pentapeptides and to identify all possible types of stable conformations. Later we shall prove the validity of this assumption.

Alanine pentapeptide AAAAA has no stable conformation since its lifetime in the most stable conformation was 2.3% of the molecular dynamics simulation time. It can be explained by a short side chain and weak interactions between them. We did not choose glycine pentapeptide GGGGG because glycine has additional conformational space of

backbone [22]. In the AAAAA sequence, the residues in the central and in two other positions were consequentially replaced with all possible canonical amino acid residues. After elimination of identical sequences, we obtained 44,860 unique sequences of pentapeptides and carried out molecular dynamics simulation for them (see Methods).

The size distribution of the two largest clusters of molecular-dynamic trajectories for 44,860 pentapeptides is shown in Figure 1. A large peak is observed in the bottom-left corner. In the bottom-right corner, there is a small peak. The local maximum of the distribution in the lower right corner corresponds to the size of the largest cluster 1 of more than 4,000 states, i.e. 80% of the conformational states under consideration (see Supplementary Table 2 for the list of pentapeptides with lifetime in stable conformation over 80%). So, the threshold of 80% of the conformational states was chosen for the criterion of structural stability. Clustering of molecular-dynamic trajectories for 44,860 pentapeptides revealed that in 1,225 pentapeptides of the largest cluster contained more than 80% of the conformational states. Thus, in the examined set of 44,860 pentapeptides, only 2.73% of them were conformationally stable. The most stable peptide was IATAE with stable conformational state 99.56% of the simulation time.

A structure and sequence of central conformation in the largest cluster was chosen for each structurally stable pentapeptide (see Materials and Methods). Further, the central conformation of stable pentapeptides was clustered using the torsion angles of the polypeptide backbone  $\phi$  and  $\psi$  resulting in 54 groups (Supplementary Table 1). The largest group contains 324 stable pentapeptides. A representative structure closest to the center of the cluster was chosen for each cluster of similar 3D structures (see representative structures and their parameters in Supplementary Table 2).

Conformationally stable pentapeptides (KDKAA, PAHVA, AAWCD, RARAY, KNGAA, PAKKA, WAEAW, KREAA, DAICA, RAMAD, EAREA, KGYAA, WAEYA, EAKAK, EKDAA, APKKA, AAPKE, APKGA, PAGAP, FDGAA, PACAK, KAKDA, EAGKA, APPAP, PDPAA, RAEAD) did not join any clusters and formed their own groups with a unique topology of the polypeptide backbone.

For description of the features of the amino acid sequences of structurally stable peptides the central residue in the pentapeptide was named as "0", and for the others "-2" (N terminus), "-1", "+1" and "+2" (C terminus) numeration was used. The balance of

ALA will not be discussed in most cases, since it is known that its amount is significantly increased in all positions.

In particular, all 322 sequences of stable peptides that fall into cluster 1 contain at position "+2" 97.8% LYS and 2.2% ARG (Table 1, also see Supplementary\_inf.xls file for details). A similar analysis carried out for cluster 2 containing 218 pentapeptides shows in 100% of cases localization at position "+2" of a residue with a negatively charged side group (ASP 78.9% and GLU 21.1%). Negatively charged residues ASP and GLU can be found at the position "-2" in the cluster 3 sequences with the probability 72.3% and 26.1% respectively. Analysis of occurrence of amino acid residues in different positions of pentapeptides for other clusters was not possible due to the small number of peptides (total 107 pentapeptides for clusters 14-54). In general, it can be seen that for each cluster of conformationally stable pentapeptides there is a characteristic pattern of the location of charged amino acid residues (Table 1).

We assumed that the possible functions of structurally rigid pentapeptides can be: the initiation of the formation of elements of the secondary structure, the maintenance of the conformation of the secondary structure, and the termination of the elements of the secondary structure. To identify structurally rigid elements that can play this role, coordinates of three N- or C-terminal C-alpha atoms were compared with idealized elements of the secondary structure. To construct idealized elements of the secondary structure, the following values of the torsion angles of the polypeptide backbone were used for  $\alpha$ -helix ( $\varphi = -57.0^\circ$ ;  $\psi = -47.0^\circ$ ), anti-parallel  $\beta$ -structure ( $\varphi = -139.0^\circ$ ;  $\psi = +135.0^\circ$ ) and parallel  $\beta$ -structure ( $\varphi = -119.0^\circ$ ;  $\psi = +113.0^\circ$ ) [22].

Supplement Table 3 shows the results of comparison of the structures of the terminal regions of rigid pentapeptides with C-alpha atoms of idealized secondary structures. In the 40 of 54 clusters the best value of RMSD were less than 0.1. In 13 clusters, the distances to the nearest idealized structures were in the range from 0.1 to 0.2. For one cluster (namely cluster 43), this distance was 0.207.

The good structural correspondence of stable pentapeptides to elements of the secondary structure of proteins is intriguing and suggests that they can play an important role in the formation of pre-folded conformation of natural polypeptide chains, by initiating and terminating conformations corresponding to the elements of the secondary

structure. Pentapeptides, the beginning and end of which correspond well to the same type of secondary structure, should be considered as peptides that maintain this type of secondary structure (Table 2). In particular, pentapeptides from clusters 3, 7, 11, 12, 13, 15, 25, 27, 28, 34, 35, 37, 38, 43, 45, 48, 51 and 52 should be considered as pentapeptides maintaining  $\alpha$ -helix. Pentapeptides from clusters 4, 8, 21, 24, 30, 32, 49 and 54 maintain the  $\uparrow\uparrow\beta$ -structure conformation. We did not find structurally stable peptides that maintain the  $\downarrow\uparrow\beta$ -structure conformation.

Table 2 roughly summarizes the behavior of each cluster as follows:

- Peptides from clusters 1, 22, 31, 44, 46 and 50 can link  $\alpha$ -helix with  $\uparrow\downarrow\beta$ -structure. Peptides from clusters 10, 16, 20, 23, 39, 42 and 47 forming the link from the  $\uparrow\downarrow\beta$ -structure to the  $\alpha$ -helix.
- Pentapeptides from the clusters 1, 2, 5, 9, 14, 18, 29, 31, 36, 41, 44, 46, 50 and 53 can make a link from  $\alpha$ -helix to  $\uparrow\uparrow\beta$ -structure. A link from  $\uparrow\uparrow\beta$ -structure to  $\alpha$ -helix can be realized by the peptides from the clusters 10, 16, 17, 19, 39, 40 and 42.
- The transition from the  $\uparrow\downarrow\beta$ -structure to the  $\uparrow\uparrow\beta$ -structure can be realized by the pentapeptides from the clusters 30 and 33, the pentapeptides realizing the transition from the  $\uparrow\uparrow\beta$  structure to the  $\uparrow\downarrow\beta$ -structure can be found in clusters 6 and 54.

The identified structurally stable pentapeptides probably form an almost complete set of topological types of peptides necessary for the formation of the prefolding state of the polypeptide chain. The replacement of the frequently used alanine residues with residues with other functional groups can substantially replenish a set of structurally stable elements, but it is unlikely to change the set of topological types found.

To understand how often conformationally stable peptides are found in native proteins, we analyzed the sequence of human Na, K-ATPase (Uniprot code P05024). The sequence of Na, K-ATPase contains 1,017 overlapping pentapeptides. Molecular modeling showed that 79 structurally stable pentapeptides were identified among them, which cover 32.4% of its sequence.

#### 4. Discussion

In this paper, in the framework of our approach [6,23], we proposed a method for searching for conformationally stable pentapeptides for protein folding. For each protein sequence, it is possible to determine conformationally stable sites of the sequence and to predict their spatial structure. Such regions in the protein structure ensure the formation of a prefolding conformational state. A "correct" pre-folding state leads to a decrease in the dimensionality of the multidimensional phase space. A simple gradient descent in such a space can quickly and unambiguously lead to natural polypeptide chains in the native spatial organization. Identification of such sites in proteins allows us to investigate the mechanism of protein folding and to make rational design of native protein sequences.

The performed research revealed topologically complete set of structures that ensures the formation of prefolding conformations for proteins of various topological types. It is important to note that among a limited number of identified types of structurally stable elements there are not only those that initiate formation or maintenance of a certain type of secondary structure, but also terminate them, ensuring the continuation of the way of the polypeptide chain in a definite solid angle.

It is of fundamental importance that 54 topological types of structurally stable pentapeptides were obtained by using in their sequence only three residues with effectively interacting functional groups. The remaining positions in the sequences of structurally stable elements occupied by ALA residues in our study may be occupied by residues that provide interactions in the later stages of folding.

It can be assumed that in real proteins, structurally stable regions can occupy a significant portion of the amino acid sequence of the protein. For example, the sequence of Na, K-ATPase (code Uniprot P05024) has 79 structurally stable pentapeptides, which cover 32.4% of its sequence. It is interesting to note that only 2.73% of the 44 860 pentapeptides studied were structurally stable.

Of further interest is the study of pentapeptides that have two conformational states and that can thus serve as "switches" at the junctions of the moving parts of proteins. Also interesting is the content of conformationally labile pentapeptides capable of adopting the structure dictated by the local environment and the course of the

polypeptide chain. In addition, it seems an interesting prospect to study the mutual arrangement of pentapeptides with different conformational properties.

### **Acknowledgements**

This study was partially supported by Russian Foundation for Basic Research (#18-54-00037) and was supported by the Program for Molecular and Cellular Biology of the Russian Academy of Sciences. The Na,K-ATPase peptides stability calculation was funded by the Russian Science Foundation (grant #14-14-01152). AdB's work was supported by grants from the Ministry of Research (France), University Paris Diderot, Sorbonne, Paris Cité (France), National Institute for Blood Transfusion (INTS, France), National Institute for Health and Medical Research (INSERM, France) and labex GR-Ex. The labex GR-Ex, reference ANR-11-LABX-0051 is funded by the program "Investissements d'avenir" of the French National Research Agency, reference ANR-11-IDEX-0005-02. AdB acknowledges to Indo-French Centre for the Promotion of Advanced Research / CEFIPRA for collaborative grant (number 5302-2).

We would also like to thanks Axel T. Brünger for the X-PLOR software license. The authors are grateful to Dr. Alexei Adzhubei for attentive reading and valuable comments.

## Legends

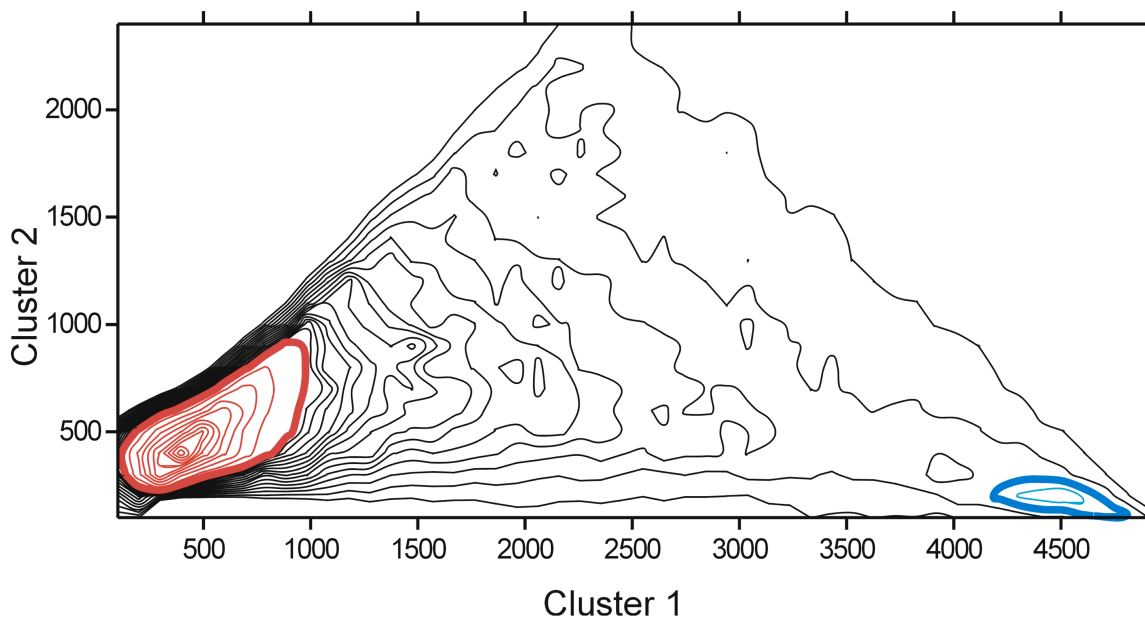


**Figure 1.** The size distribution of the two largest clusters of conformation states of molecular-dynamic trajectories for 44,860 pentapeptides. Structurally unstable peptides are located on the inside of the red line in the bottom-left corner (bold red isoline 300, thin 100). Structurally stable peptides are located inside of the blue line in the bottom-right corner (bold blue isoline 40, thin 20).

## References

- [1] Y. Hatakeyama, T. Sawada, M. Kawano, M. Fujita, Conformational preferences of short peptide fragments, *Angew. Chem. Int. Ed Engl.* 48 (2009) 8695–8698. doi:10.1002/anie.200903563.
- [2] A.V. Batyanovskii, P.K. Vlasov, Short protein segments with prevalent conformation, *Biophysics.* 53 (2009) 264–267. doi:10.1134/S0006350908040040.
- [3] B.K. Ho, K.A. Dill, Folding Very Short Peptides Using Molecular Dynamics, *PLOS Comput. Biol.* 2 (2006) e27. doi:10.1371/journal.pcbi.0020027.
- [4] A. g. de Brevern, C. Etchebest, S. Hazout, Bayesian probabilistic approach for predicting backbone structures in terms of protein blocks, *Proteins Struct. Funct. Bioinforma.* 41 (2000) 271–287. doi:10.1002/1097-0134(20001115)41:3<271::AID-PROT10>3.0.CO;2-Z.
- [5] A.G. de Brevern, C. Benros, R. Gautier, H. Valadié, S. Hazout, C. Etchebest, Local backbone structure prediction of proteins, *In Silico Biol.* 4 (2004) 381–386.
- [6] A.N. Nekrasov, Entropy of Protein Sequences: An Integral Approach, *J. Biomol. Struct. Dyn.* 20 (2002) 87–92. doi:10.1080/07391102.2002.10506825.
- [7] C. Etchebest, C. Benros, S. Hazout, A.G. de Brevern, A structural alphabet for local protein structures: Improved prediction methods, *Proteins Struct. Funct. Bioinforma.* 59 (2005) 810–827. doi:10.1002/prot.20458.
- [8] M. Tyagi, A.G. de Brevern, N. Srinivasan, B. Offmann, Protein structure mining using a structural alphabet, *Proteins.* 71 (2008) 920–937. doi:10.1002/prot.21776.
- [9] A.P. Joseph, N. Srinivasan, A.G. de Brevern, Improvement of protein structure comparison using a structural alphabet, *Biochimie.* 93 (2011) 1434–1445. doi:10.1016/j.biochi.2011.04.010.
- [10] S. Léonard, A.P. Joseph, N. Srinivasan, J.-C. Gelly, A.G. de Brevern, mulPBA: an efficient multiple protein structure alignment method based on a structural alphabet, *J. Biomol. Struct. Dyn.* 32 (2014) 661–668. doi:10.1080/07391102.2013.787026.
- [11] S. Mahajan, G. Agarwal, M. Iftikhar, B. Offmann, A.G. de Brevern, N. Srinivasan, DoSA: Database of Structural Alignments, *Database J. Biol. Databases Curation.* 2013 (2013) bat048. doi:10.1093/database/bat048.
- [12] A.P. Joseph, H. Valadié, N. Srinivasan, A.G. de Brevern, Local structural differences in homologous proteins: specificities in different SCOP classes, *PloS One.* 7 (2012) e38805. doi:10.1371/journal.pone.0038805.
- [13] I. Vetrivel, S. Mahajan, M. Tyagi, L. Hoffmann, Y.-H. Sanejouand, N. Srinivasan, A.G. de Brevern, F. Cadet, B. Offmann, Knowledge-based prediction of protein backbone conformation using a structural alphabet, *PloS One.* 12 (2017) e0186215. doi:10.1371/journal.pone.0186215.
- [14] M. Tyagi, A. Bornot, B. Offmann, A.G. de Brevern, Protein short loop prediction in terms of a structural alphabet, *Comput. Biol. Chem.* 33 (2009) 329–333. doi:10.1016/j.compbiolchem.2009.06.002.
- [15] A. Bornot, C. Etchebest, A.G. de Brevern, Predicting protein flexibility through the prediction of local structures, *Proteins.* 79 (2011) 839–852. doi:10.1002/prot.22922.
- [16] D. Brevern, A. G. A. Bornot, P. Craveur, C. Etchebest, J.-C. Gelly, PredyFlexy: flexibility and local structure prediction from sequence, *Nucleic Acids Res.* 40 (2012) W317–W322. doi:10.1093/nar/gks482.

- [17] D.A. Case, T.E. Cheatham, T. Darden, H. Gohlke, R. Luo, K.M. Merz, A. Onufriev, C. Simmerling, B. Wang, R.J. Woods, The Amber biomolecular simulation programs, *J. Comput. Chem.* 26 (2005) 1668–1688. doi:10.1002/jcc.20290.
- [18] J.W. Ponder, D.A. Case, Force fields for protein simulations, *Adv. Protein Chem.* 66 (2003) 27–85.
- [19] G.V. Nikiforovich, Computational molecular modeling in peptide drug design, *Int. J. Pept. Protein Res.* 44 (1994) 513–531. doi:10.1111/j.1399-3011.1994.tb01140.x.
- [20] S. Rahmanov, I. Kulakovskiy, L. Uroshlev, V. Makeev, Empirical potentials for ion binding in proteins, *J. Bioinform. Comput. Biol.* 8 (2010) 427–435.
- [21] P.H.A. Sneath, R.R. Sokal, Numerical taxonomy. The principles and practice of numerical classification., *Numer. Taxon. Princ. Pract. Numer. Classif.* (1973). <https://www.cabdirect.org/cabdirect/abstract/19730310919> (accessed January 18, 2019).
- [22] G.E. Schulz, R.H. Schirmer, Prediction of Secondary Structure from the Amino Acid Sequence, in: *Princ. Protein Struct.*, Springer, New York, NY, 1979: pp. 108–130. doi:10.1007/978-1-4612-6137-7\_6.
- [23] A.N. Nekrasov, A.A. Anashkina, A.A. Zinchenko, A new paradigm of protein structural organization, Institute of Physics, Belgrade, 2014. [https://www.researchgate.net/profile/Alexei\\_Nekrasov/publication/270684947\\_A\\_New\\_Paradigm\\_of\\_Protein\\_Structural\\_Organization/links/54b285da0cf220c63cd25c21.pdf#page=15](https://www.researchgate.net/profile/Alexei_Nekrasov/publication/270684947_A_New_Paradigm_of_Protein_Structural_Organization/links/54b285da0cf220c63cd25c21.pdf#page=15) (accessed March 24, 2016).

Table 1. Sequence patterns of conformationally stable pentapeptides of clusters 1-13. X is any amino acid residue.

Cluster	Number of sequences	Representative amino acid residue				
		-2	-1	0	1	2
1	324	A/X	A/X	X	A/X	K/R
2	216	A/X	A	X	A	D/E
3	186	D/E	A/K/R	E/D/W/Y	A	A
4	92	R/K	A/K/R	X	A/E/D	A/K/R
5	86	N/A/K/R	A	X	A	E/D
6	41	R/K	E/D	X	A	A
7	38	K/R	A/X	G/X	A	A
8	29	A	A	P	A/X	K/R
9	28	D/E	A	X	A	P
10	28	K/R	A/D/E	P	A	A
11	18	D/E	A	X	A	R/K
12	17	K/R	A/P	X	A/R	A
13	15	D/E	X	X	A	A
14-54	107	A/P/K/R/E/D	A/P/D/E	R/K/E/D/G/P	A/K/R	A/D/E/K/R/P

Table 2. Clusters of conformationally stable pentapeptides that maintain the elements of the secondary structure and provide a transition from one type of secondary structure to another.

		N-termini of pentapeptide		
		Terminate the $\alpha$ -helix	Terminate the $\uparrow\downarrow\beta$ -structure	Terminate the $\uparrow\uparrow\beta$ -structure
C-termini of pentapeptide	Initiate the $\alpha$ -helix	3, 7, 11, 12, 13, 15, 25, 27, 28, 34, 35, 37, 38, 43, 45, 48, 51, 52	10, 16, 20, 23, 39, 42, 47	10, 16, 17, 19, 39, 40, 42
	Initiate the $\uparrow\downarrow\beta$ -structure	1, 22, 31, 44, 46, 50	-	6, 54
	Initiate the $\uparrow\uparrow\beta$ -structure	1, 2, 5, 9, 14, 18, 29, 31, 36, 41, 44, 46, 50, 53	30, 33	4, 8, 21, 24, 30, 32, 49, 54

## Supplement. Molecular dynamics protocol.

A fragment of the command file of the X-PLOR program, describing the initial minimization of the starting conformation, and the MD protocol for the simulation of pentapeptides are given below.

```
minimize powell
  nstep=500           { THE NUMBER OF MINIMIZATION STEP }
  nprint=1
  drop=10.
end

{ CONTROL CONFORMATION & ENERGY TERMS }

  write coordinates output=test.pdb end
  system

display $zero $ENER $VDW $ELEC $DIHE

{ END OF OUTPUT CONTROL }

print threshold=0.1 bonds
print threshold=10.0 angles
print threshold=0.0 cdihedrals

{ MOLECULAR DYNAMICS CYCLE }

  set seed=432324368 end

  vector do (vx=maxwell(300.)) (all)
  vector do (vy=maxwell(300.)) (all)
  vector do (vz=maxwell(300.)) (all)

  vector do (fbeta=100.) (all)

evaluate ($nucycl=10000)
evaluate ($time_step=1)

while($nucycl>0) loop md_cycle_1

{ MOLECULAR DYNAMICS }

dynamics verlet
  nstep=1000
  time=0.001
  nprint=999
  ntrfrq=200
  tbath=300.
  tcoupling=true
  firsttemp=300.
  finaltemp=300.
  iasvelocity=maxwell
```

```

end

{ CONTROL CONFORMATION & ENERGY TERMS }

write coordinates output=test.pdb end { Write out coordinates }
system

evaluate($num_print=$num_print+1)
display $num_print $ENER $VDW $ELEC $DIHE

{ END OF OUTPUT CONTROL }

evaluate($nucycl=$nucycl-$time_step)

end loop md_cycle_1

```

**Supplementary Table 1.** Sequences of pentapeptides for each of 54 structural clusters formed by pentapeptides with stable spatial conformation.

Cluster number	Sequences	Conformational stability by molecular dynamics simulation trajectories, (% of the conformational states)
<b>Cluster 1</b>		
	AAMVK	81.8
	AVVAK	88.8
	ASCAK	86.4
	AAFFK	93.2
	AALFK	90.1
	FAYAK	89.9
	AAYYK	91.9
	ALSAK	83.5
	AAFLK	89.3
	AHQAK	80.4
	YAIK	86.2
	AQYAK	85.1
	AVNAK	84.8
	TAWAK	87.2
	AWQAK	84.1
	AALWK	89.2
	LAWAK	88.8
	VAVAK	90.5
	AALLK	82.6
	ALHAK	84.1
	AHFAK	87.8
	LAAAK	87.5
	LAFK	90.8
	AALAK	87.7
	AACSK	83.2

	AAWKK	85.0
	VATAK	80.7
	LAIK	80.1
	AAWHK	87.7
	AFMAK	90.9
	AVIAK	85.6
	FAVAK	83.4
	AAHMK	88.7
	AAMYK	89.9
	AIYAK	89.1
	AYYAK	84.9
	AWAAK	95.0
	FASAK	83.4
	AANWK	87.5
	AMVAK	83.7
	FATAK	88.1
	HAHAK	82.6
	AACWK	86.8
	AAIAK	80.0
	TAHAK	92.0
	AMLAK	87.5
	AAVAK	87.6
	AAIHK	91.6
	ANKAK	92.2
	AWHAK	90.4
	AQSAK	82.8
	AFVAK	90.6
	AAMFK	88.4
	FAHAK	89.7
	AAVLK	82.7
	LASAK	87.0
	ACTAK	86.7
	AAWAK	81.2
	AFTAK	81.5
	ATSAK	81.6
	AAVNK	83.7
	AYMAK	84.3
	ATHAK	92.1
	AMTAK	85.1
	ACHAK	85.9
	AALHK	84.4
	ATVAK	81.0
	AFSAK	88.9
	AFIAK	93.8
	YAVAK	81.7
	AAIYK	85.6
	AAVIK	83.3
	LAVAK	88.7
	AAQRK	81.5
	ACVAK	88.3

	AAAFK	92.4
	ALLAK	80.0
	LAYAK	87.5
	AVWAK	89.8
	AYHAK	85.4
	AIFAK	97.4
	MAAAK	82.2
	AAYFK	88.9
	AFFAK	91.6
	AAHWK	88.3
	AATIK	87.8
	MAMAK	81.9
	AFQAK	82.8
	ALCAK	84.2
	AAYLK	95.1
	AWVAK	91.6
	AVAAK	88.9
	TASAK	88.9
	ACIAK	89.0
	ALVAK	81.1
	AAISK	90.0
	ALTAK	81.1
	AATCK	80.9
	AASYK	81.7
	AVTAK	91.0
	AWFAK	95.9
	YASAK	81.1
	TAMAK	86.8
	VALAK	85.8
	FALAK	90.2
	AAMWK	82.2
	ASLAK	87.8
	LATAK	81.4
	AASFK	88.7
	ACCAK	82.2
	WALAK	86.7
	YAWAK	90.3
	CAVAK	89.9
	FAFAK	89.9
	YAMAK	89.4
	CAHAK	83.9
	VASAK	90.4
	YAQAK	89.2
	SAMAK	85.5
	ATLAK	90.1
	YALAK	92.6
	MAFAK	81.1
	IAIAK	94.7
	WAHAK	81.7
	AAQWK	82.5

	ASFAK	90.9
	WAIKAK	82.6
	IYAK	91.5
	TAQAK	89.7
	LALAK	85.0
	IWAK	88.9
	AFLAK	88.2
	YAAK	88.4
	WAVAK	82.7
	VAMAK	81.3
	AATWK	87.7
	LAMAK	87.1
	AALYK	89.2
	AMFAK	89.8
	SALAK	81.7
	AWWAK	80.2
	AYLAK	94.6
	ACWAK	86.1
	ATTAK	92.6
	AANHK	80.5
	MAYAK	87.5
	VAFK	88.4
	AAQCK	84.9
	ASYAK	91.6
	AATYK	81.1
	AAIMK	90.5
	ASSAK	85.1
	ASVAK	89.8
	AAILK	87.8
	AACVK	86.9
	ACQAK	89.5
	AATAK	82.8
	AATLK	88.6
	AIKAK	95.5
	AAWLK	95.0
	AAFIK	93.3
	AAICK	83.3
	ALWAK	89.3
	AARQK	90.9
	AAMLK	90.7
	ACLAK	86.9
	AAQVK	85.8
	AAIK	84.8
	ASHAK	93.3
	AALCK	89.0
	AAWVK	92.7
	AAAYK	82.6
	AFYAK	91.5
	ACSAK	85.0
	ACYAK	85.8



	ANFAK	80.4
	AAVHK	83.4
	AYTAK	85.7
	AICAK	90.4
	AITAK	90.6
	IANAK	80.3
	AFAAK	92.3
	AHTAK	81.6
	WAAAK	86.5
	AYIAK	88.2
	CAFAK	90.6
	AAMHK	84.9
	AACFK	80.2
	FAAAK	88.5
	AAWWK	83.9
	AAFSK	86.9
	AANTK	88.7
	AAVVK	84.1
	AAMSK	85.2
	AAFTK	87.5
	KACAK	84.4
	TAFAK	80.2
	AAWMK	89.7
	AALMK	82.0
	TALAK	83.2
	AAALK	86.8
	TAYAK	83.8
	RAAAK	86.9
	AAVTK	83.6
	ACFAK	90.7
	AAIQK	88.3
	AAARK	80.0
	QAYAK	86.9
	AAVMK	83.0
	AATFK	88.8
	AAQFK	89.0
	AAHTK	85.1
	AAIVK	87.1
	AAINK	83.7
	AACTK	89.3
	WAQAK	80.9
	AAVRK	84.8
	AAIKK	87.4
	AAVQK	85.6
	AAITK	83.4
	AALRK	87.5
	AASKK	83.1
	AAMTK	83.7
	AACKK	80.4
	AARKK	84.0

	AACRK	86.9
	RAMAK	95.6
	AAYRK	83.2
	AAHKK	86.7
	AAVMK	84.5
	AASMK	80.1
	AAHFK	85.5
	AATKK	81.1
	AALKK	88.0
	AYSAK	81.1
	AAVYK	89.8
	AAAQK	83.8
	ATYAK	87.7
	WATAK	80.8
	WAFAK	87.6
	AARLK	90.1
	IASAK	94.6
	SAFAK	84.3
	IALAK	87.8
	AFWAK	82.9
	SAAAK	83.9
	MAVAK	83.3
	CATAK	81.4
	AALSK	81.3
	AAHHK	82.3
	AASIK	84.5
	AAAHK	88.4
	AAHRK	80.1
	AMWAK	81.6
	YATAK	93.4
	CAIAK	90.3
	PAEAK	88.8
	AAFRK	81.6
	YAFAK	90.6
	AAFVK	82.3
	AALVK	85.4
	YACAK	81.8
	ATFAK	89.4
	AAFKK	90.9
	AASRK	83.0
	EAVAR	81.5
	EATAR	83.5
	AALRR	80.3
	AAVRR	81.9
	TAFAR	81.1
	AAATK	84.0
	KAMAK	86.9
	KAIAK	94.7
	IATAK	88.5
<b>Cluster 2</b>		

	AWMAD	89.6
	ASMAD	81.7
	AVLAD	94.6
	TAMAD	93.8
	CANAD	88.0
	ATIAD	90.2
	AIYAD	91.6
	ALLAD	82.6
	FAAAD	92.7
	HASAD	92.8
	AYHAD	86.3
	CAFAD	86.8
	ALFAD	88.1
	SASAD	89.4
	AMEAD	80.1
	AADHD	88.6
	AQIAD	85.8
	ALYAD	84.3
	AVMAD	89.1
	YAAAD	86.9
	YANAD	94.6
	IAIAD	91.8
	NACAD	86.6
	TAIAD	83.3
	HAVAD	90.7
	FANAD	92.6
	HAMAD	91.1
	WANAD	92.8
	ATFAD	82.0
	VATAD	81.9
	AMFAD	94.3
	AMMAD	82.4
	TAAAD	96.4
	AAAYLD	91.6
	QAFAD	87.4
	ASFAD	90.6
	AQVAD	81.8
	FAHAD	82.6
	AMSAD	92.0
	AYLAD	88.0
	ASSAD	91.7
	HANAD	84.4
	IALAD	94.7
	CATAD	85.4
	TASAD	93.6
	TAVAD	94.0
	TAWAD	84.6
	FAFAD	81.9
	AAFLD	82.9
	MANAD	95.3

	IADAD	92.3
	MASAD	91.5
	FATAD	91.9
	LATAD	91.9
	AHTAD	83.8
	ARMAD	86.3
	YATAD	85.2
	AEWAD	93.1
	ACVAD	95.4
	AWWAD	92.7
	VAYAD	82.9
	VACAD	84.8
	SAIAD	91.9
	AHQAD	86.5
	MACAD	95.2
	AAVCD	86.9
	AWEAD	93.4
	AWFAD	81.9
	AFIAD	87.4
	FAYAD	86.5
	NATAD	93.0
	YAYAE	80.4
	FAQAD	92.0
	YAHAE	84.3
	WAVAE	93.9
	MAHAD	85.5
	WAVAD	90.1
	MAQAD	83.5
	TAFAD	95.5
	YAQAD	81.8
	MAFAD	84.0
	WAMAD	92.1
	YAIAD	90.6
	WAYAD	92.8
	WAIAD	95.1
	WAAAD	91.9
	NAVAD	88.2
	IAWAD	89.2
	AADCD	80.1
	AFDAD	84.5
	AADQD	85.7
	ASDAD	85.9
	AMTAD	81.7
	CAYAD	83.1
	AADND	83.6
	FADAD	95.2
	AAEQD	81.2
	AYDAD	85.6
	ALDAD	82.3
	SACAD	80.3

	AWCAD	93.8
	AADGD	87.8
	PAWAD	84.8
	AIVAD	82.3
	AATTD	82.5
	AISAD	90.2
	AALLD	84.7
	AFMAD	92.4
	AQLAD	85.3
	AATSD	83.5
	AWAAD	85.9
	ALMAD	81.2
	AFVAD	81.9
	AAVSD	86.6
	ALWAD	83.2
	AFCAD	88.0
	AYMAD	96.7
	ALIAD	92.0
	AYVAD	81.1
	AIMAD	86.7
	AQFAD	87.0
	IAAAD	90.2
	AASYD	81.8
	AAMCD	81.6
	SAWAD	84.7
	PAHAD	84.6
	AALTD	85.9
	AATYD	87.0
	AANAD	85.5
	AAQHD	80.8
	AAYMD	83.0
	AAIHD	80.8
	AAMVD	81.5
	AAFVD	92.6
	AAVTD	81.2
	AAYTD	85.2
	APSAD	93.4
	ANDAD	80.9
	AAFTD	90.4
	AWDAD	88.1
	AAVID	81.3
	AACHD	85.2
	RAFAE	80.1
	MADAD	93.3
	AADID	85.2
	QAMAD	80.1
	YAFAD	82.6
	YALAD	86.7
	NAYAD	88.4
	IASAD	85.1

	WATAD	97.4
	IACAD	82.6
	FAMAD	85.8
	AVFAD	88.5
	AWIAD	92.6
	IAQAD	82.3
	WAQAD	82.5
	WACAD	97.8
	QALAD	84.6
	WAWAD	98.0
	FASAD	93.6
	LAMAD	80.3
	FAIAD	81.4
	MAFAE	84.9
	TAFAE	89.2
	MAHAE	91.0
	MANAE	91.9
	NAWAE	88.2
	AMIAE	81.6
	YALAE	82.2
	MALAE	88.1
	WATAE	95.6
	NANAE	94.6
	YACAE	89.7
	HAHAE	91.9
	WAHAE	95.3
	HADAE	87.7
	AYCAE	81.5
	MAIAE	89.5
	NANAD	91.5
	WADAD	93.1
	WAYAE	86.2
	WAWAE	97.5
	VAMAE	80.5
	WADAE	85.6
	WASAE	94.4
	WAMAE	80.4
	WAIAE	92.4
	IAVAE	85.1
	QAVAE	81.6
	MAVAE	88.7
	QAHAE	84.0
	TADAE	86.8
	VALAD	82.1
	YAVAD	90.9
	YAWAD	87.4
	YAMAD	93.9
	WASAD	82.7
	YAHAD	81.1
	HAMAE	82.7

	DANAE	94.2
	RAVAE	87.5
	RAYAE	94.6
	TATAE	84.4
	IAQAE	91.3
	NAMAE	85.6
	RAMAE	87.0
	RAIAE	87.3
	AWVAE	81.5
	RAWAE	89.4
	APSAE	84.8
	APYAE	97.4
	APNAE	96.9
	APLAD	86.7
	ARIAD	81.8
	AADFD	91.0
<b>Cluster 3</b>		
	DALAS	85.5
	DASAF	81.8
	DAWAN	90.7
	DAFAC	90.6
	DWWAA	83.1
	DRQAA	90.7
	DATAT	80.3
	DAWAT	89.5
	DAWAL	82.3
	DAEAT	94.6
	DAEWA	95.1
	DTEAA	97.0
	DAEAL	82.8
	EAWAA	80.3
	DAWAH	89.9
	EAWAC	87.6
	DACAQ	82.2
	DALAN	81.6
	DADAL	82.7
	DAVAC	86.8
	DADAT	80.4
	DALAC	81.8
	DAMAC	81.6
	DNHAA	80.5
	DAIAS	81.9
	DAWAM	86.1
	DALAH	83.0
	DYWAA	86.1
	DAYAF	80.8
	DCWAA	82.2
	DSYAA	89.6
	DAYWA	80.4
	DASAT	87.1

	DAIAC	81.1
	DSEAA	93.3
	DAEAH	94.4
	DCEAA	93.0
	DLEAA	90.8
	DVEAA	82.8
	DYEAA	93.4
	EMEAA	82.9
	DWEAA	87.8
	DIEAA	88.1
	DATAM	80.7
	DACAH	84.6
	DAIAT	88.6
	DATAC	82.8
	DAEAQ	96.4
	DAYAT	83.3
	DAAAH	85.8
	DASAH	89.6
	DACAC	89.9
	DQEAA	91.9
	DAEAM	95.1
	DFEAA	93.5
	DAAAQ	84.0
	DAMAH	95.2
	DHCAA	81.3
	DAAAL	85.6
	DANAH	94.1
	DAFAH	82.2
	DAHAH	85.9
	DHHAA	80.7
	DAYAS	80.3
	DALAY	80.7
	DHNAA	81.7
	DEWAA	87.3
	DAMAN	81.8
	DEYAA	82.8
	DEDAA	86.5
	DEIAA	83.3
	DAVAS	81.1
	DAQAS	83.4
	DQWAA	81.5
	DAWYA	83.3
	DHWAA	88.4
	DAWAQ	80.7
	EKGAA	86.7
	DAMFA	81.5
	DAAAS	82.2
	DKTAA	94.1
	DKFAA	97.3
	DAFVA	80.7

	DAYVA	86.4
	EAWAS	86.8
	DHLAA	87.0
	DAWAC	96.8
	EKLAA	89.5
	ERHAA	93.7
	DAFAT	88.3
	EAEAH	85.2
	EAEAM	96.0
	DAEVA	81.8
	DAEAI	88.9
	DAEYA	94.0
	EASAK	82.3
	DAENA	88.2
	DAELA	82.2
	DAECA	86.4
	DAEIA	89.9
	EKQAA	85.8
	EAEAY	88.3
	DAEAV	84.5
	DAEQA	88.6
	DAEAA	86.4
	DAEMA	94.9
	DMEAA	90.0
	DAEAC	98.7
	EAEAV	80.8
	EAEAS	98.3
	EAEQA	86.4
	EAEAA	87.3
	EAENA	84.4
	EAEHA	88.8
	ECEAA	88.0
	EFEAA	92.8
	EAEAD	80.7
	EIEAA	89.2
	EAEVA	86.8
	EAEIA	87.5
	EAWAT	86.8
	EAEYA	83.2
	ECWAA	80.1
	DAEAF	96.1
	EAEAI	82.3
	EAEAT	87.8
	EAEAF	80.5
	ERQAA	88.0
	ESEAA	88.2
	EYEAA	91.1
	EAWHA	85.0
	EKFAA	91.6
	EAWIA	82.5

	EAWAM	86.8
	EAWSA	80.6
	DAEAN	93.3
	DKKAA	82.5
	DRFAA	87.2
	DRSAA	89.0
	DRAAA	93.0
	DRTAA	96.4
	DKVAA	92.4
	DKCAA	91.9
	DKWAA	98.7
	DKYAA	94.6
	DAMAF	85.3
	DKQAA	92.0
	DAWAS	94.8
	DKLAA	97.5
	DADAC	92.1
	DAESA	93.3
	DAEAS	98.8
	DAYAC	90.9
	DFWAA	83.9
	DAEFA	91.8
	DAEHA	96.7
	DKHAA	97.4
	DAAAC	83.8
	DALAT	90.5
	DRIAA	91.0
	DRNAA	96.8
	DRGAA	81.0
	DRYAA	93.7
	DAWIA	82.6
	DRVAA	99.3
	DRMAA	87.5
	DKMAA	96.0
	DKAAA	97.5
	EKSAA	93.2
	DKSAA	96.5
	EEQAA	84.4
	EAESA	92.2
	EAEAQ	93.4
	HAEAE	90.8
	EETAA	81.1
	DEVAA	91.1
	KADAE	94.8
	KAEAE	95.3
	RAEAE	80.0
	EATAK	93.5
	EKNAA	85.4
	EKAAA	93.9
	EKCAA	86.6

	EKHAA	88.9
	DKRAA	86.5
	KRDAA	88.9
<b>Cluster 4</b>		
	RAHAK	96.6
	RLLAA	85.8
	RATAK	89.8
	KAFAK	89.8
	KATAK	90.6
	RAYAK	96.1
	RWWAA	85.7
	RRCAA	90.0
	RAWAK	97.0
	RKMAA	90.4
	RRIAA	90.4
	KAYAK	93.8
	RASAR	80.8
	RKFAA	94.3
	RLIAA	86.4
	RASAK	84.0
	RAQAK	91.5
	RALAR	95.3
	KAWAK	93.6
	KKWAA	81.4
	KRFAA	95.7
	KAVAK	96.0
	RKCAA	86.0
	RKSAA	93.0
	PAIRA	85.1
	RYIAA	86.8
	RFFAA	88.3
	RRSAA	90.7
	RRFAA	87.6
	RRAAA	97.1
	RIVAA	81.8
	RAFAR	99.0
	RYFAA	86.1
	RKNAA	84.7
	RAVAK	92.8
	RRRAA	89.2
	RARAK	90.6
	RRYAA	85.5
	RKIAA	87.9
	RKTAA	90.6
	RVVAA	80.2
	RAADA	88.3
	RATSA	83.9
	RLFAA	84.6
	KAIAR	86.2
	KARAR	90.9

	RKLAA	95.3
	KKLAA	97.0
	RKAAA	95.4
	RRVAA	98.8
	KALAK	84.6
	KKTAA	88.8
	KAHAK	93.8
	KKCAA	91.3
	KKFAA	91.7
	RAHAR	83.7
	RVMAA	85.0
	RAKEA	85.8
	RAWAR	89.3
	REFAA	87.9
	TKIAA	90.0
	PKEAA	93.0
	PAWRA	82.6
	ANEDA	80.9
	EALDA	84.3
	EAVDA	95.1
	EACEA	81.4
	EAYEA	85.1
	EATEA	89.7
	MEFAA	81.4
	TEFAA	84.7
	EAMEA	83.2
	YAKEA	91.0
	EARIA	94.5
	NACEA	80.7
	WELAA	88.2
	WENAA	88.8
	HEFAA	81.1
	MEMAA	82.2
	EAAEA	91.0
	DARCA	82.0
	DAFEA	96.3
	KAKAE	92.1
	NKEAA	80.7
	WNDAA	89.4
	WKEAA	82.4
	WHEAA	92.7
	WNEAA	94.0
	WADAA	86.0
	WCDAA	80.3
	WIDAA	89.1
	RAEAK	93.6
<b>Cluster 5</b>		
	KAFAD	89.5
	RATAD	93.0
	NAFAD	86.7

	KAWAE	82.5
	QATAD	97.0
	RAYAD	93.5
	RAQAD	95.2
	RAIAD	96.2
	EAYAD	83.3
	MAYAD	95.2
	QAYAD	83.1
	KAAAD	85.4
	NAIAD	88.5
	SATAD	89.8
	KAVAD	98.8
	HAFAD	96.0
	VAWAD	81.6
	QASAD	95.0
	HAQAD	92.0
	IAFAE	86.4
	RAWAD	96.9
	KATAE	88.6
	RAHAD	96.5
	KASAD	91.0
	RALAD	95.1
	RASAD	96.1
	MALAD	97.6
	KACAD	92.0
	RAFAD	87.8
	KAMAD	98.2
	RANAD	81.2
	NAAAD	90.2
	NASAD	96.2
	NADAD	91.3
	NAMAD	89.5
	LAYAD	95.6
	FASAE	80.2
	VAFAE	89.0
	VALAE	82.7
	AANNE	82.9
	SATAE	85.3
	KAHAD	90.3
	QAFAE	97.8
	KASAE	84.2
	QAIAE	94.4
	NAIAE	98.8
	IASAE	97.4
	LALAE	98.8
	AAHRE	91.0
	IACAE	98.2
	IAWAE	98.0
	TAHAE	95.3
	HALAE	95.3

	NAYAE	91.1
	TAWAE	96.2
	CALAE	87.1
	AAMRE	90.0
	ASYAE	87.2
	IATAE	99.6
	FAMAE	87.1
	NACAE	85.7
	TANAE	96.6
	EAYAE	98.9
	QAQAE	89.0
	TACAE	96.4
	NAWAD	96.5
	KALAD	84.2
	TATAD	97.9
	NATAE	90.4
	EAI AE	93.0
	VANAE	93.7
	HAIAD	88.5
	RAVAD	92.5
	NAHAD	83.8
	HAAAD	87.3
	TASAE	88.1
	HADAD	92.7
	AAFRE	80.4
	AAQRE	91.7
	AACKE	88.3
	AASRE	88.0
	AAYRE	91.7
	IAIAE	84.2
	TAIAE	91.9
	AAMKE	92.3
	AARRE	95.8
<b>Cluster 6</b>		
	KEHAA	85.6
	KECAA	85.9
	KESAA	90.3
	KELAA	87.7
	KEWAA	86.3
	REQAA	90.4
	REMAA	91.6
	REWAA	95.2
	RECAA	95.6
	KEMAA	93.0
	REVAA	89.0
	REHAA	91.3
	REIAA	90.5
	RESAA	96.6
	KENAA	81.9
	KAFEA	81.6

	KAMEA	87.9
	KEQAA	86.2
	KEFAA	91.9
	KEIAA	91.0
	KAREA	95.1
	RENAA	96.3
	REAAA	98.2
	REYAA	90.6
	RETAA	81.3
	RDAAA	91.6
	RDWAA	97.7
	RDMAA	96.6
	RDCAA	92.6
	RDVAA	98.6
	KEVAA	88.8
	KAIEA	93.7
	RDFAA	82.8
	RDSAA	92.8
	RDIAA	90.9
	RD TAA	97.9
	KAQEA	87.7
	KDIAA	87.3
	KAECA	84.3
	REGAA	84.5
	KEGAA	84.8
<b>Cluster 7</b>		
	KRYAA	86.1
	KYYAA	81.4
	KALWA	98.3
	KAYIA	93.4
	KAIAA	80.1
	KAF AI	94.6
	KAGAH	82.9
	KAGLA	86.0
	KAGAY	83.5
	KFGAA	87.1
	KHGAA	81.6
	KLYAA	93.0
	KWVAA	96.5
	KFCAA	83.4
	KAIVA	96.5
	KMGAA	83.9
	KFYAA	96.3
	KL GAA	81.5
	KWGAA	84.0
	RFYAA	93.1
	KT LAA	94.2
	RQVAA	89.3
	KAI AW	96.7
	KAGAL	89.7

	RMIAA	86.1
	KSFAA	91.6
	RAWYA	88.8
	RAWIA	93.3
	RALAC	90.1
	RAILA	82.7
	RALAV	87.3
	KAGAI	84.0
	RRGAA	80.1
	RKGAA	87.6
	RAGIA	82.8
	RALAY	87.0
	RAEEA	90.2
	NAIEA	94.9
<b>Cluster 8</b>		
	FAPAK	81.2
	AAPIK	90.8
	AAPSK	89.7
	VAPAK	90.4
	AAPCK	83.4
	LAPAK	80.1
	ASPAK	81.8
	AAPRK	87.7
	AAPTK	91.3
	AAPQK	80.6
	ARPAK	87.3
	AHPAK	81.8
	AAPYK	88.0
	AAPMK	81.1
	AAPHK	87.4
	AVPAK	80.8
	AAPKK	86.7
	ARRAK	88.6
	AFPAR	83.7
	TAPAK	87.3
	AAPQR	80.1
	CAPAK	80.8
	AAPLK	86.2
	AYPAK	92.4
	AKQAK	80.1
	AKWAR	87.8
	AKTAK	80.2
	AKPAK	83.0
	AKVAK	90.2
<b>Cluster 9</b>		
	DANAP	94.9
	DAAAP	92.8
	DATAP	95.5
	DAVAP	92.5
	DAHAP	94.5

	DACAP	91.0
	DAWAP	82.5
	EAYAP	92.2
	DARAP	89.7
	EALAP	90.4
	DAYAP	95.8
	DAFAP	91.3
	DALAP	95.6
	EASAP	92.4
	DAQAP	98.1
	EAFAP	91.5
	EAIAP	88.2
	EAMAP	93.1
	EAAAP	80.7
	DASAP	89.9
	DAMAP	93.7
	EAHAP	85.5
	EAVAP	93.0
	EANAP	94.6
	APEAP	84.7
	EWIAA	80.1
	APYRA	83.1
	EARAR	86.5
<b>Cluster 10</b>		
	WDPAA	92.8
	RAPMA	83.3
	KAPMA	83.6
	APPEA	80.8
	RAPIA	80.7
	RAPWA	95.0
	RNPAA	87.6
	RAPAS	84.3
	RAPAE	93.2
	KNPAA	82.7
	KAPTA	85.1
	RAPPA	92.5
	RAPYA	86.3
	KAPPA	95.7
	DDRAA	91.5
	EDKAA	92.1
	KDDAA	87.5
	KAYPA	97.2
	KEPAA	83.9
	KAQAR	86.2
	KAPAD	92.1
	KWEAA	88.0
	KVEAA	91.2
	KDTAA	84.5
	KEYAA	99.0
	KDMAA	94.6

	KDYAA	97.5
	KDFAA	82.3
<b>Cluster 11</b>		
	DAIAR	84.1
	DAYAR	90.0
	DAHAK	96.8
	DAQAR	80.9
	DACAK	92.6
	DATAR	89.2
	DAVAR	93.8
	DANAR	81.3
	EAWAR	97.6
	DALAR	86.4
	DAFAK	90.5
	DASAR	85.7
	DATAK	89.0
	DAIAK	93.0
	DAWAR	89.7
	DVCAA	83.4
	DDFAA	92.9
	EACAK	89.0
<b>Cluster 12</b>		
	KAKRA	88.8
	KIKAA	81.8
	KAKYA	91.6
	KPTAA	90.9
	KATRA	82.4
	KAKKA	99.0
	RPKAA	86.7
	KPQAA	90.5
	KPYAA	90.7
	KACRA	89.8
	RPHAA	84.3
	KPFAA	92.7
	RAKRA	88.7
	RAHRA	89.8
	EPPAA	93.2
	KPNAA	91.1
	KALRA	81.8
<b>Cluster 13</b>		
	DAKAI	86.6
	ESQAA	97.2
	DAKAN	91.3
	DAKAC	94.0
	DAKAM	82.3
	ECYAA	94.8
	ECFAA	95.8
	DAQNA	85.1
	DFIAA	95.7
	DLFAA	99.3

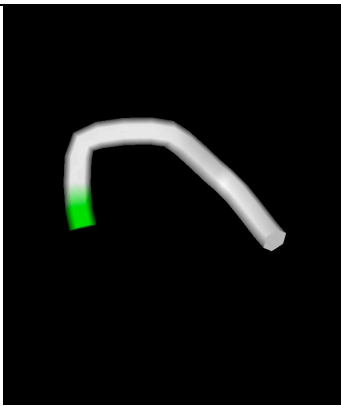
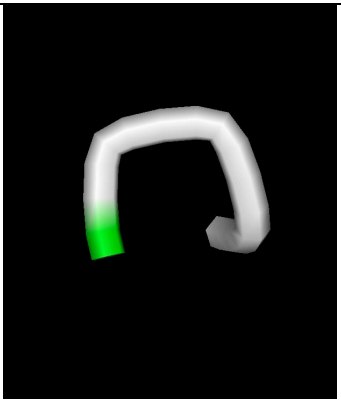
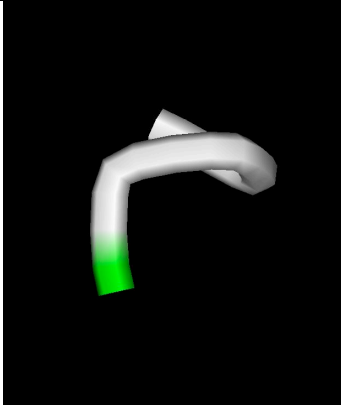
	DCMAA	96.5
	DGYAA	83.0
	DGRAA	88.6
	DGKAA	88.0
	DGHAA	87.0
<b>Cluster 14</b>		
	AARKS	81.3
	AARKI	81.3
	VARKA	87.7
	AIRKA	80.4
	AWRKA	86.5
	AAKKF	80.7
	AAKRV	82.5
	ADRWA	83.6
	AERFA	82.9
	IDRAA	83.1
	AAKRR	82.4
	EARPA	83.3
	RDRAA	88.3
<b>Cluster 15</b>		
	APWAD	93.8
	APQAD	95.0
	APYAD	91.5
	APPAD	80.7
	APRAE	91.6
	APKAE	96.8
	APWAE	92.3
	APIAE	96.5
	APEAK	94.7
	APPAE	91.5
<b>Cluster 16</b>		
	ADRQA	84.6
	ADKHA	81.1
	ADKAT	84.2
	ADRRRA	87.0
	VEKAA	82.8
	ADRAL	83.2
	ADRTA	82.7
	RKRAA	84.0
	KKRAA	94.5
	RRKAA	90.7
<b>Cluster 17</b>		
	PADTA	85.8
	PYDAA	83.3
	PADWA	86.6
	PADAW	83.4
	PADAM	83.3
	PADAY	85.3
	PADEA	89.1
	PRDAA	82.4

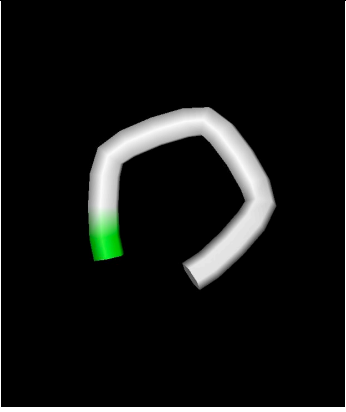
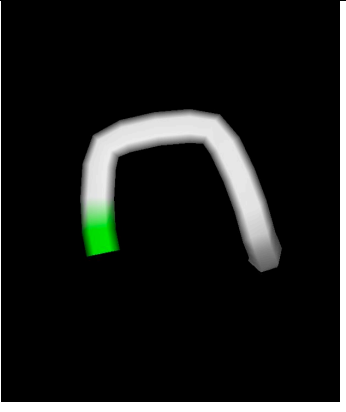
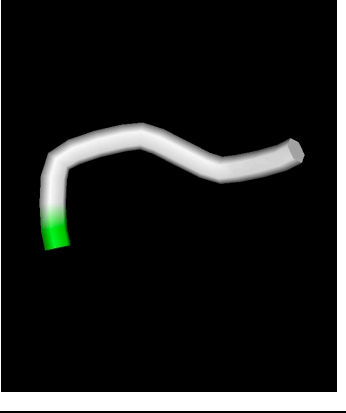
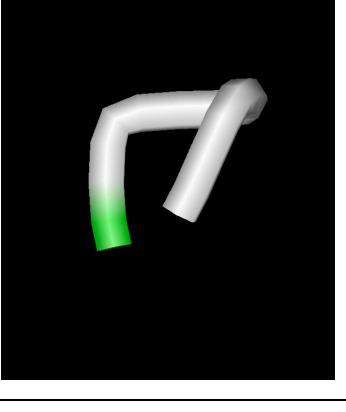
	PAEEA	84.6
<b>Cluster 18</b>		
	KANAR	82.0
	KAAAR	80.5
	KAFAR	85.8
	KAVRA	80.2
	KASRA	89.8
	ADQAP	82.0
	ACEAP	81.4
	AYEAP	82.4
	AHEAP	81.5
<b>Cluster 19</b>		
	APGTA	80.2
	APGVA	80.3
	APGLA	83.7
	APGCA	80.9
	TPGAA	81.3
	APGMA	85.6
<b>Cluster 20</b>		
	PDNAA	82.0
	PDTAA	94.6
	PDAAA	82.1
	PDIAA	84.8
<b>Cluster 21</b>		
	EAHAW	81.3
	NAEAW	85.4
	EAIK	99.5
<b>Cluster 22</b>		
	RAEAW	87.5
	DAKKA	90.5
	KAWEA	85.1
<b>Cluster 23</b>		
	NDIAA	81.9
	NDCAA	84.6
	HDFAA	85.6
<b>Cluster 24</b>		
	APPAR	88.0
	APPAK	80.5
	DAPAK	89.5
<b>Cluster 25</b>		
	AACDD	80.8
	AANDD	81.5
<b>Cluster 26</b>		
	AEHRA	84.9
	AENKA	86.8
<b>Cluster 27</b>		
	APEAE	81.1
	APDRA	82.9
<b>Cluster 28</b>		
	DARGA	81.6

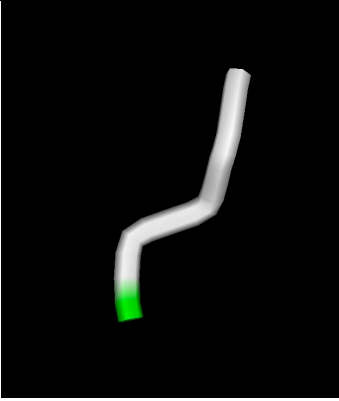
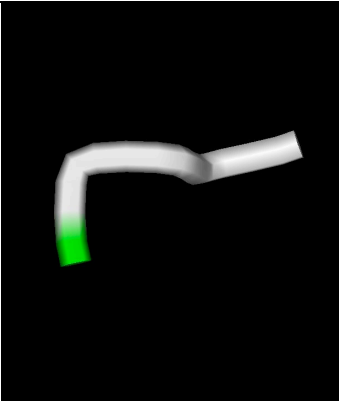
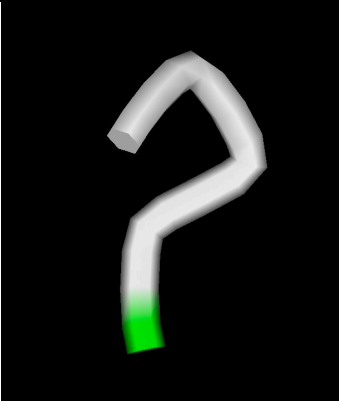
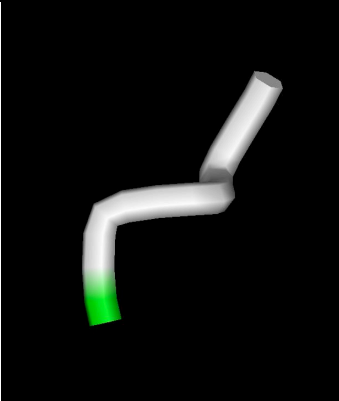
	DARQA	93.9
<b>Cluster 29</b>		
	EKDAA	84.0
<b>Cluster 30</b>		
	PAGAP	80.8
<b>Cluster 31</b>		
	KNGAA	84.6
<b>Cluster 32</b>		
	APPAP	82.6
<b>Cluster 33</b>		
	KAKDA	87.5
<b>Cluster 34</b>		
	EAREA	86.1
<b>Cluster 35</b>		
	WAEYA	81.0
<b>Cluster 36</b>		
	PAKKA	82.6
<b>Cluster 37</b>		
	KGYAA	87.7
<b>Cluster 38</b>		
	AAWCD	81.9
<b>Cluster 39</b>		
	KDKAA	90.8
<b>Cluster 40</b>		
	PAHVA	83.9
<b>Cluster 41</b>		
	RARAY	81.0
<b>Cluster 42</b>		
	AAPKE	92.8
<b>Cluster 43</b>		
	APKGA	81.3
<b>Cluster 44</b>		
	EAKAK	95.4
<b>Cluster 45</b>		
	FDGAA	84.0
<b>Cluster 46</b>		
	WAEAW	81.3
<b>Cluster 47</b>		
	PDPAA	83.7
<b>Cluster 48</b>		
	RAMAD	94.5
<b>Cluster 49</b>		
	KREAA	80.3
<b>Cluster 50</b>		
	PACAK	80.1
<b>Cluster 51</b>		
	DAICA	81.8
<b>Cluster 52</b>		
	RAEAD	86.2
<b>Cluster 53</b>		

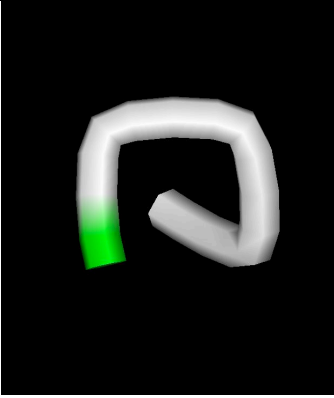
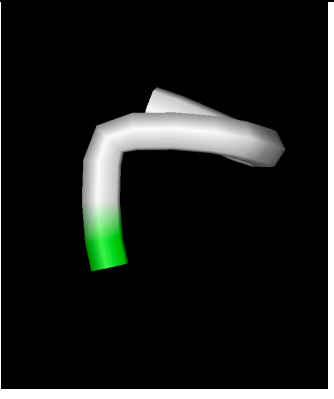
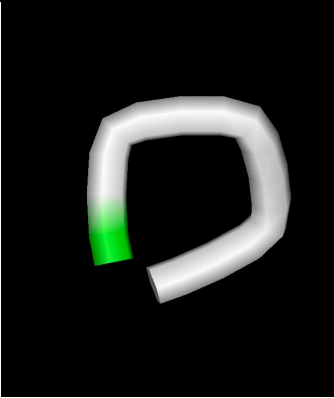
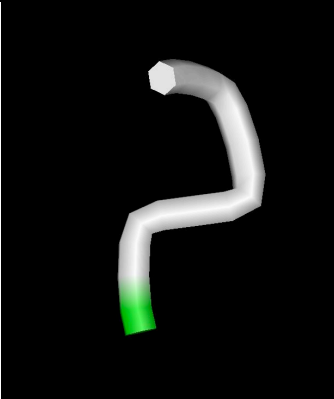
	APKKA	82.3
<b>Cluster 54</b>		
	EAGKA	86.6

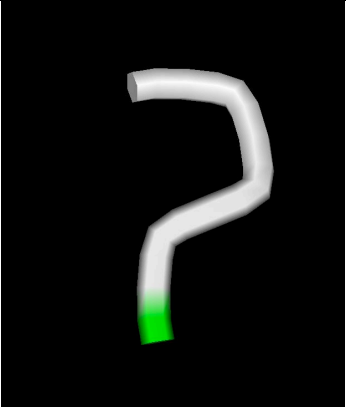
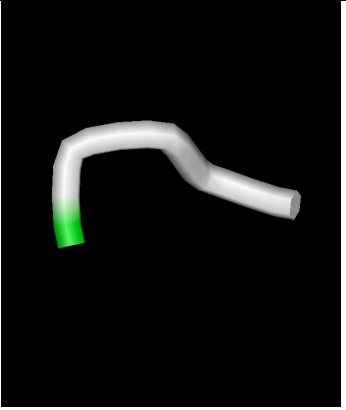
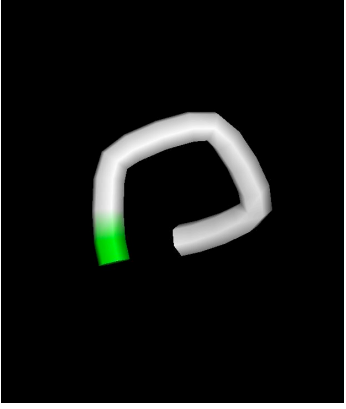
**Supplementary Table 2.** 54 structural clusters formed by pentapeptides with stable spatial conformation. C $\alpha$ -atoms of the first amino acid residue from the N-terminus is highlighted in green, and the C $\alpha$  atoms of the first three N-terminal amino acid residues of pentapeptide are located in the vertical plane.

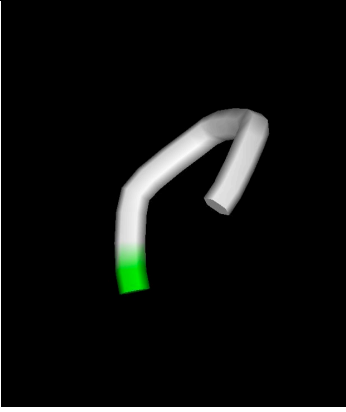
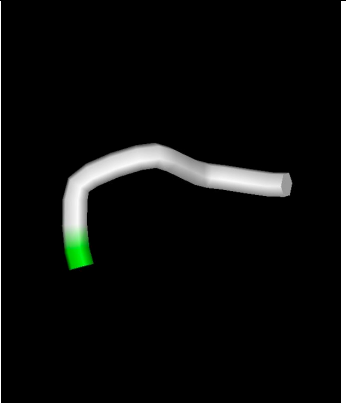
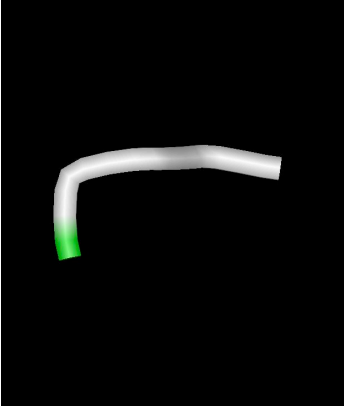
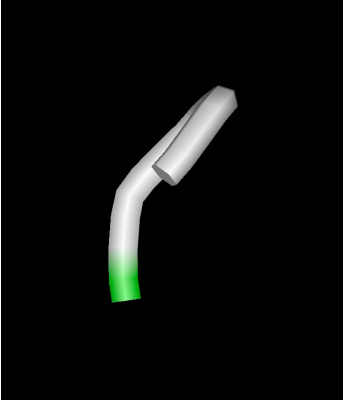
Cluster number	The sequence of the representative pentapeptide structure	Number of elements in a cluster	Торсионные углы $\phi$ и $\psi$ центр. ИЕ		Representative spatial structure of the cluster. N-terminus is highlighted in green. The first three N-terminal C $\alpha$ -atoms are located in the vertical plane.
1	AALFK	324	$\psi$ 1	-28.8	
			$\phi$ 2	-81.9	
			$\psi$ 2	-44.9	
			$\phi$ 3	-97.2	
			$\psi$ 3	156.1	
			$\phi$ 4	-80.4	
			$\psi$ 4	156.1	
			$\phi$ 5	-123.	
2	AWMAD	216	$\psi$ 1	85.8	
			$\phi$ 2	-99.3	
			$\psi$ 2	-39.7	
			$\phi$ 3	-121.1	
			$\psi$ 3	44.4	
			$\phi$ 4	-155.3	
			$\psi$ 4	44.4	
			$\phi$ 5	-137.0	
3	DALAS	186	$\psi$ 1	135.8	
			$\phi$ 2	-138.3	
			$\psi$ 2	22.7	
			$\phi$ 3	-105.6	
			$\psi$ 3	-14.1	
			$\phi$ 4	-110.6	
			$\psi$ 4	-14.1	
			$\phi$ 5	-113.5	

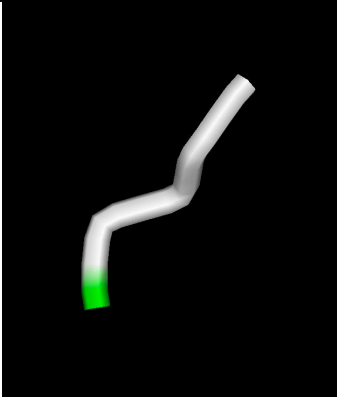
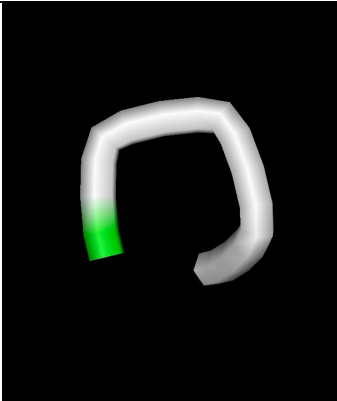
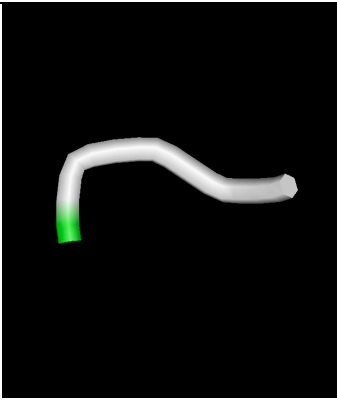
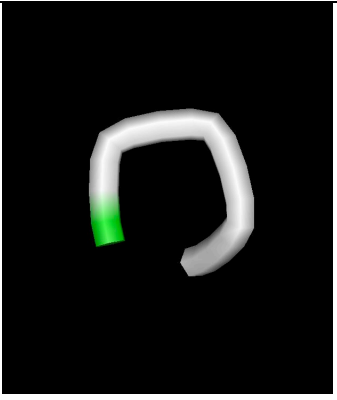
4	RAHAK	92	$\psi 1$	108.0	
			$\varphi 2$	-117.4	
			$\psi 2$	-66.5	
			$\varphi 3$	-109.6	
			$\psi 3$	-51.1	
			$\varphi 4$	-110.9	
			$\psi 4$	-51.1	
			$\varphi 5$	-120.8	
5	KAFAD	86	$\psi 1$	-60.8	
			$\varphi 2$	-99.9	
			$\psi 2$	-45.7	
			$\varphi 3$	-137.0	
			$\psi 3$	61.5	
			$\varphi 4$	-159.7	
			$\psi 4$	61.5	
			$\varphi 5$	-129.2	
6	KEHAA	41	$\psi 1$	-53.0	
			$\varphi 2$	-124.6	
			$\psi 2$	-53.6	
			$\varphi 3$	-139.4	
			$\psi 3$	169.6	
			$\varphi 4$	-122.2	
			$\psi 4$	169.6	
			$\varphi 5$	-93.9	
7	KRYAA	38	$\psi 1$	127.0	
			$\varphi 2$	-113.0	
			$\psi 2$	54.5	
			$\varphi 3$	68.7	
			$\psi 3$	-38.3	
			$\varphi 4$	-87.5	
			$\psi 4$	-38.3	
			$\varphi 5$	-92.2	

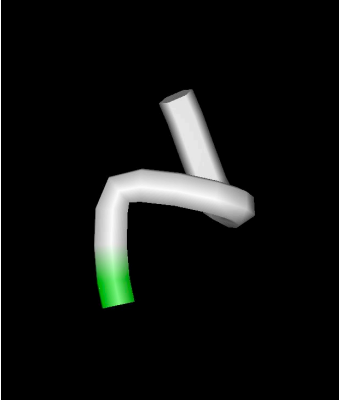
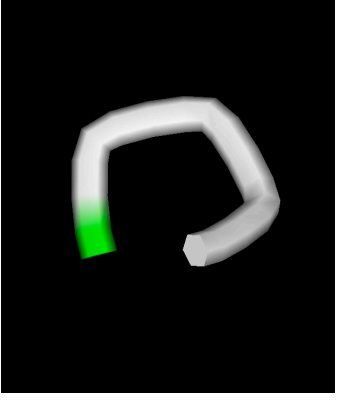
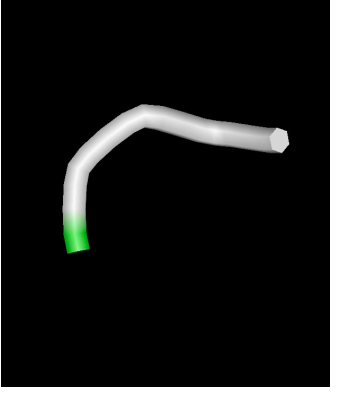
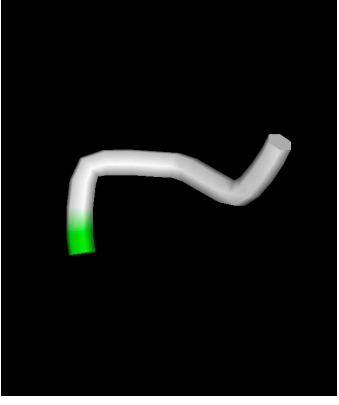
8	FAPAK	29	$\psi 1$	-56.9	
			$\phi 2$	-89.8	
			$\psi 2$	129.0	
			$\phi 3$	-67.7	
			$\psi 3$	137.9	
			$\phi 4$	-79.8	
			$\psi 4$	137.9	
			$\phi 5$	-121.2	
9	DANAP	28	$\psi 1$	166.3	
			$\phi 2$	-106.4	
			$\psi 2$	-8.9	
			$\phi 3$	-94.1	
			$\psi 3$	100.5	
			$\phi 4$	-119.4	
			$\psi 4$	100.5	
			$\phi 5$	-82.2	
10	WDPAA	28	$\psi 1$	133.6	
			$\phi 2$	-101.5	
			$\psi 2$	144.5	
			$\phi 3$	-81.1	
			$\psi 3$	-20.4	
			$\phi 4$	-104.4	
			$\psi 4$	-20.4	
			$\phi 5$	-131.0	
11	DAIAR	18	$\psi 1$	143.2	
			$\phi 2$	-135.8	
			$\psi 2$	23.7	
			$\phi 3$	-104.1	
			$\psi 3$	53.9	
			$\phi 4$	-106.2	
			$\psi 4$	53.9	
			$\phi 5$	-132.0	

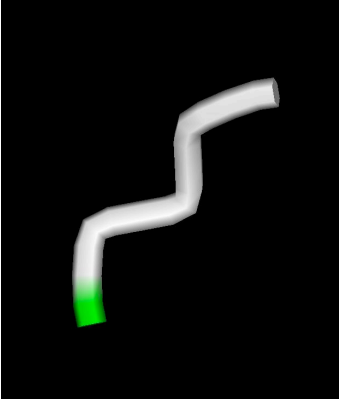
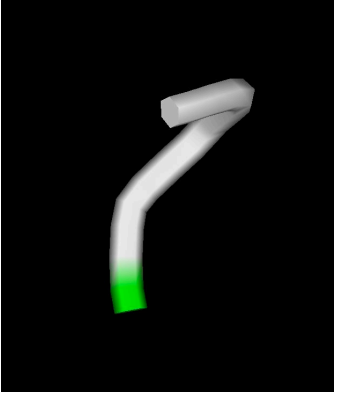
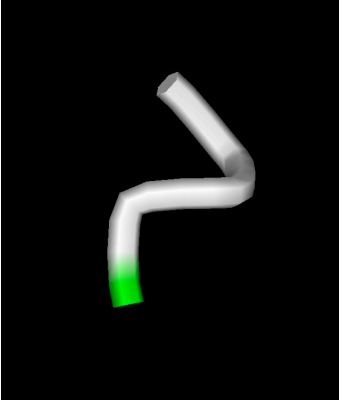
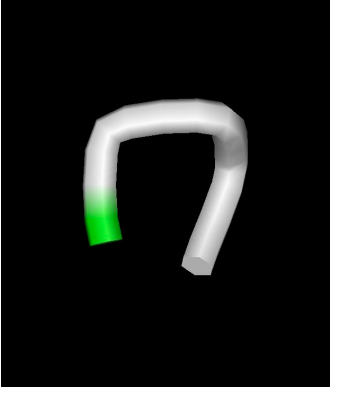
12	KAKRA	17	$\psi 1$	97.3	
			$\varphi 2$	-72.9	
			$\psi 2$	-38.7	
			$\varphi 3$	-83.6	
			$\psi 3$	-39.2	
			$\varphi 4$	-67.1	
			$\psi 4$	-39.2	
			$\varphi 5$	-106.8	
13	DAKAI	15	$\psi 1$	-54.8	
			$\varphi 2$	71.6	
			$\psi 2$	35.0	
			$\varphi 3$	-130.9	
			$\psi 3$	-31.7	
			$\varphi 4$	-109.0	
			$\psi 4$	-31.7	
			$\varphi 5$	-110.8	
14	AARKS	13	$\psi 1$	-37.5	
			$\varphi 2$	-88.9	
			$\psi 2$	-38.4	
			$\varphi 3$	-73.1	
			$\psi 3$	-53.0	
			$\varphi 4$	-112.9	
			$\psi 4$	-53.0	
			$\varphi 5$	-107.4	
15	APWAD	10	$\psi 1$	124.6	
			$\varphi 2$	-67.0	
			$\psi 2$	108.6	
			$\varphi 3$	-97.8	
			$\psi 3$	27.0	
			$\varphi 4$	-143.7	
			$\psi 4$	27.0	
			$\varphi 5$	-141.1	

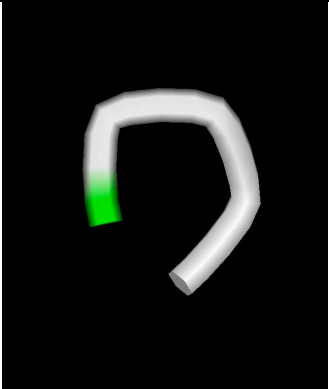
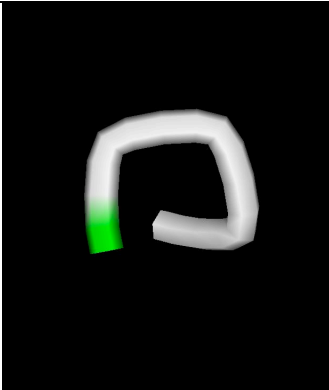
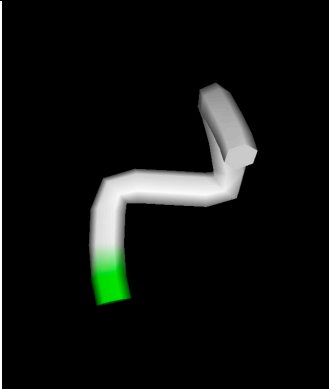
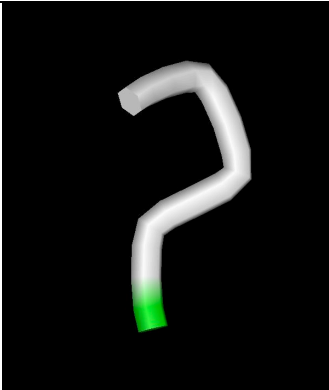
16	ADRQA	10	$\psi 1$	-58.1	
			$\phi 2$	-83.1	
			$\psi 2$	145.7	
			$\phi 3$	-130.4	
			$\psi 3$	-40.0	
			$\phi 4$	-100.3	
			$\psi 4$	-40.0	
			$\phi 5$	-109.5	
17	PADTA	9	$\psi 1$	-47.0	
			$\phi 2$	-147.4	
			$\psi 2$	49.2	
			$\phi 3$	-149.6	
			$\psi 3$	-27.8	
			$\phi 4$	-99.5	
			$\psi 4$	-27.8	
			$\phi 5$	-124.5	
18	KANAR	9	$\psi 1$	13.7	
			$\phi 2$	-92.3	
			$\psi 2$	-45.7	
			$\phi 3$	-86.9	
			$\psi 3$	116.7	
			$\phi 4$	-92.4	
			$\psi 4$	116.7	
			$\phi 5$	-98.4	
19	APGTA	6	$\psi 1$	118.8	
			$\phi 2$	-68.6	
			$\psi 2$	124.6	
			$\phi 3$	126.0	
			$\psi 3$	-50.7	
			$\phi 4$	-99.6	
			$\psi 4$	-50.7	
			$\phi 5$	-137.1	

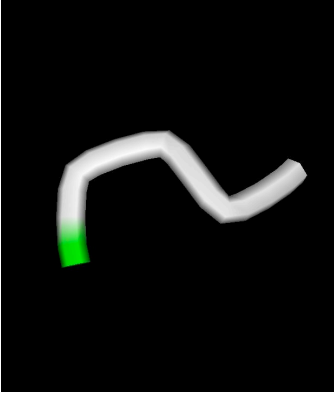
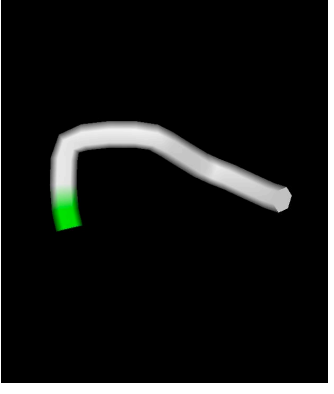
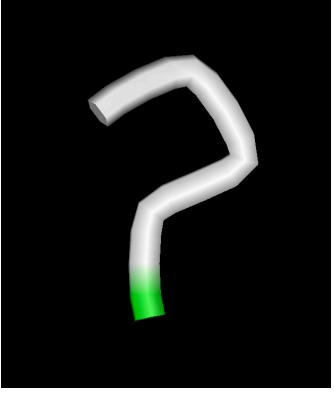
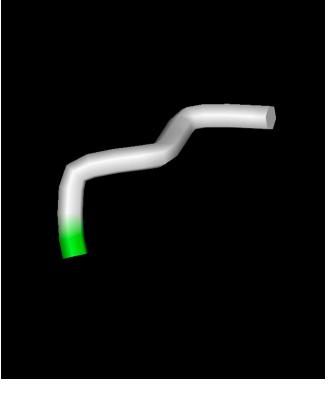
20	PDNAA	4	$\psi 1$	58.5	
			$\phi 2$	-154.5	
			$\psi 2$	-112.8	
			$\phi 3$	-129.7	
			$\psi 3$	-48.4	
			$\phi 4$	-98.2	
			$\psi 4$	-48.4	
			$\phi 5$	-114.9	
21	EAHAW	3	$\psi 1$	-62.1	
			$\phi 2$	-154.2	
			$\psi 2$	-44.7	
			$\phi 3$	-97.7	
			$\psi 3$	127.6. 2	
			$\phi 4$	-97.1	
			$\psi 4$	127.6	
			$\phi 5$	-114.5	
22	RAEAW	3	$\psi 1$	112.0	
			$\phi 2$	-141.4	
			$\psi 2$	-20.4	
			$\phi 3$	-79.0	
			$\psi 3$	173.2	
			$\phi 4$	-138.8	
			$\psi 4$	173.2	
			$\phi 5$	-115.9	
23	NDIAA	3	$\psi 1$	-50.2	
			$\phi 2$	-147.3	
			$\psi 2$	-142.6	
			$\phi 3$	-113.4	
			$\psi 3$	-44.2	
			$\phi 4$	-110.4	
			$\psi 4$	-44.2	
			$\phi 5$	-117.3	

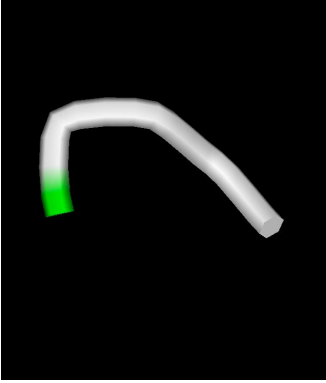
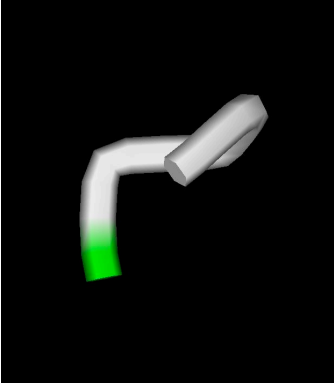
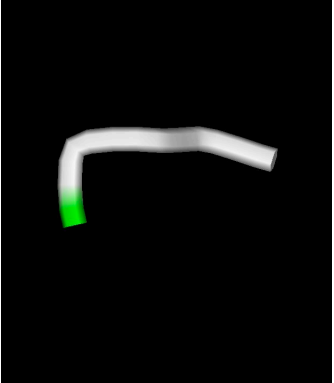
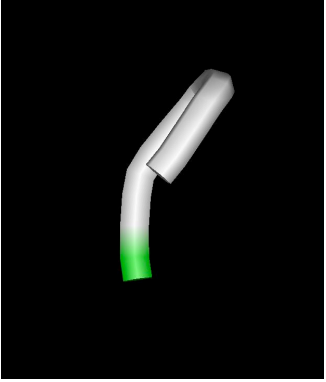
24	APPAR	3	$\psi 1$	114.7	
			$\phi 2$	-71.9	
			$\psi 2$	135.2	
			$\phi 3$	-70.1	
			$\psi 3$	123.4	
			$\phi 4$	-94.8	
			$\psi 4$	123.4	
			$\phi 5$	-143.1	
25	AACDD	2	$\psi 1$	80.2	
			$\phi 2$	-92.1	
			$\psi 2$	-48.9	
			$\phi 3$	-128.3	
			$\psi 3$	5.4	
			$\phi 4$	-114.2	
			$\psi 4$	5.4	
			$\phi 5$	-95.1	
26	AEHRA	2	$\psi 1$	97.8	
			$\phi 2$	-114.9	
			$\psi 2$	-48.9	
			$\phi 3$	-142.1	
			$\psi 3$	170.7	
			$\phi 4$	-101.9	
			$\psi 4$	170.7	
			$\phi 5$	-103.1	
27	APEAE	2	$\psi 1$	96.9	
			$\phi 2$	-70.5	
			$\psi 2$	-0.8	
			$\phi 3$	-75.7	
			$\psi 3$	11.5	
			$\phi 4$	-119.6	
			$\psi 4$	11.5	
			$\phi 5$	-96.9	

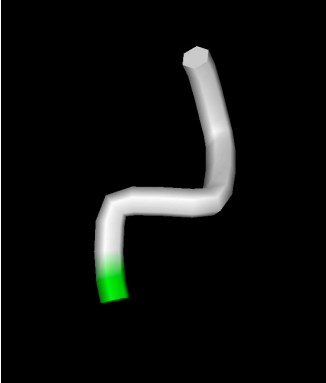
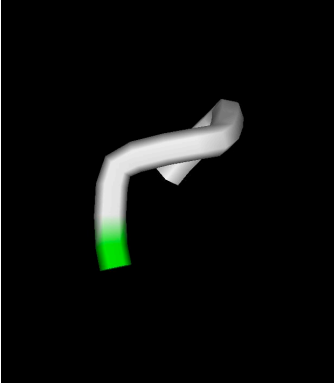
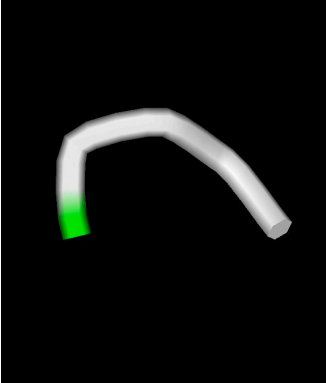
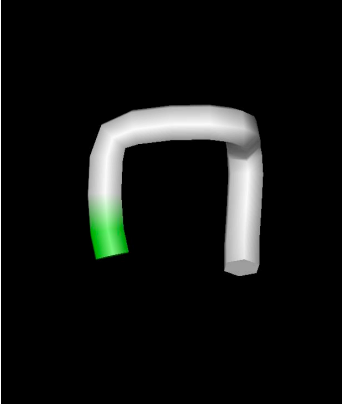
28	DARGA	2	$\psi 1$	143.1	
			$\varphi 2$	-93.2	
			$\psi 2$	-14.7	
			$\varphi 3$	-95.1	
			$\psi 3$	-62.8	
			$\varphi 4$	112.0	
			$\psi 4$	-62.8	
			$\varphi 5$	-140.3	
29	EKDAA	1	$\psi 1$	-175.8	
			$\varphi 2$	-108.2	
			$\psi 2$	-41.2	
			$\varphi 3$	-136.2	
			$\psi 3$	-43.9	
			$\varphi 4$	-151.5	
			$\psi 4$	-43.9	
			$\varphi 5$	-149.9	
30	PAGAP	1	$\psi 1$	-112.4	
			$\varphi 2$	-120.6	
			$\psi 2$	146.4	
			$\varphi 3$	85.8	
			$\psi 3$	123.1	
			$\varphi 4$	-95.0	
			$\psi 4$	123.1	
			$\varphi 5$	-78.1	
31	KNGAA	1	$\psi 1$	-47.7	
			$\varphi 2$	-122.5	
			$\psi 2$	22.9	
			$\varphi 3$	112.4	
			$\psi 3$	145.2	
			$\varphi 4$	-97.3	
			$\psi 4$	145.2	
			$\varphi 5$	-103.2	

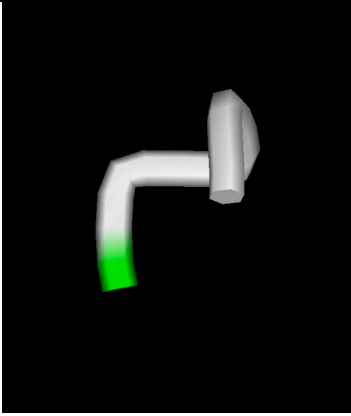
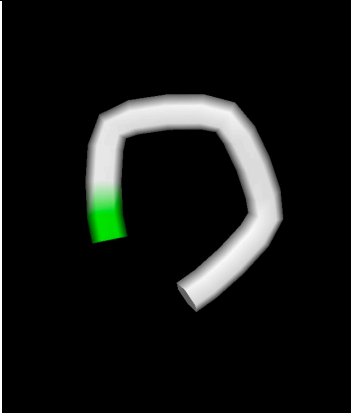
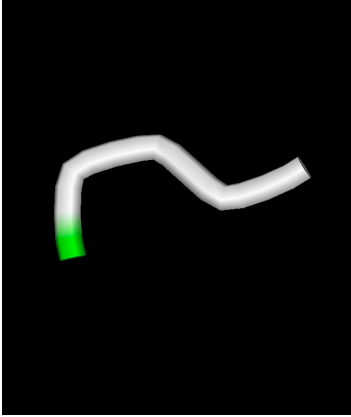
32	APPAP	1	$\psi 1$	116.7	
			$\phi 2$	-77.3	
			$\psi 2$	113.3	
			$\phi 3$	-76.6	
			$\psi 3$	109.6	
			$\phi 4$	-129.7	
			$\psi 4$	109.6	
			$\phi 5$	-70.0	
33	KAKDA	1	$\psi 1$	127.8	
			$\phi 2$	-127.0	
			$\psi 2$	-140.3	
			$\phi 3$	-103.2	
			$\psi 3$	-85.3	
			$\phi 4$	-93.5	
			$\psi 4$	-85.3	
			$\phi 5$	-97.8	
34	EAREA	1	$\psi 1$	3.4	
			$\phi 2$	-107.6	
			$\psi 2$	60.1	
			$\phi 3$	-111.9	
			$\psi 3$	11.1	
			$\phi 4$	-126.3	
			$\psi 4$	11.1	
			$\phi 5$	-134.5	
35	WAEYA	1	$\psi 1$	68.7	
			$\phi 2$	-113.4	
			$\psi 2$	-20.3	
			$\phi 3$	-92.7	
			$\psi 3$	42.1	
			$\phi 4$	74.8	
			$\psi 4$	42.1	
			$\phi 5$	-113.5	

36	PAKKA	1	$\psi 1$	-144.7	
			$\phi 2$	-78.8	
			$\psi 2$	-39.9	
			$\phi 3$	-74.2	
			$\psi 3$	-78.6	
			$\phi 4$	-107.8	
			$\psi 4$	-78.6	
			$\phi 5$	-98.5	
37	KGYAA	1	$\psi 1$	-26.6	
			$\phi 2$	101.9	
			$\psi 2$	-69.8	
			$\phi 3$	-98.0	
			$\psi 3$	-32.3	
			$\phi 4$	-83.2	
			$\psi 4$	-32.3	
			$\phi 5$	-85.9	
38	AAWCD	1	$\psi 1$	-58.8	
			$\phi 2$	-106.0	
			$\psi 2$	-10.2	
			$\phi 3$	61.0	
			$\psi 3$	23.9	
			$\phi 4$	-124.1	
			$\psi 4$	23.9	
			$\phi 5$	-143.1	
39	KDKAA	1	$\psi 1$	-143.6	
			$\phi 2$	-67.3	
			$\psi 2$	162.8	
			$\phi 3$	-125.5	
			$\psi 3$	-25.9	
			$\phi 4$	-99.2	
			$\psi 4$	-25.9	
			$\phi 5$	-133.7	

40	PAHVA	1	$\psi 1$	85.2	
			$\phi 2$	-124.2	
			$\psi 2$	-60.3	
			$\phi 3$	-111.7	
			$\psi 3$	-70.5	
			$\phi 4$	78.6	
			$\psi 4$	-70.5	
			$\phi 5$	-99.7	
41	RARAY	1	$\psi 1$	-21.4	
			$\phi 2$	-113.1	
			$\psi 2$	9.8	
			$\phi 3$	-145.1	
			$\psi 3$	127.3	
			$\phi 4$	-91.7	
			$\psi 4$	127.3	
			$\phi 5$	-114.7	
42	AAPKE	1	$\psi 1$	-30.6	
			$\phi 2$	-102.3	
			$\psi 2$	132.6	
			$\phi 3$	-86.2	
			$\psi 3$	-5.2	
			$\phi 4$	-141.0	
			$\psi 4$	-5.2	
			$\phi 5$	-123.4	
43	APKGA	1	$\psi 1$	144.7	
			$\phi 2$	-71.3	
			$\psi 2$	103.6	
			$\phi 3$	-129.5	
			$\psi 3$	-76.6	
			$\phi 4$	110.0	
			$\psi 4$	-76.6	
			$\phi 5$	-130.1	

44	EAKAK	1	$\psi 1$	166.8	
			$\varphi 2$	-88.1	
			$\psi 2$	-35.4	
			$\varphi 3$	-103.5	
			$\psi 3$	157.9	
			$\varphi 4$	-84.7	
			$\psi 4$	157.9	
			$\varphi 5$	-130.1	
45	FDGAA		$\psi 1$	109.8	
			$\varphi 2$	-107.1	
			$\psi 2$	-33.3	
			$\varphi 3$	140.1	
			$\psi 3$	-50.8	
			$\varphi 4$	-94.4	
			$\psi 4$	-50.8	
			$\varphi 5$	-110.5	
46	WAEAW	1	$\psi 1$	53.3	
			$\varphi 2$	-115.8	
			$\psi 2$	-2.0	
			$\varphi 3$	-98.7	
			$\psi 3$	143.5	
			$\varphi 4$	-118.2	
			$\psi 4$	143.5	
			$\varphi 5$	-122.0	
47	PDPAW	1	$\psi 1$	57.2	
			$\varphi 2$	-157.6	
			$\psi 2$	-170.3	
			$\varphi 3$	-71.5	
			$\psi 3$	-39.5	
			$\varphi 4$	-115.6	
			$\psi 4$	-39.5	
			$\varphi 5$	-111.4	

48	RAMAD	1	$\psi 1$	-46.9	
			$\phi 2$	60.7	
			$\psi 2$	53.7	
			$\phi 3$	-115.8	
			$\psi 3$	35.9	
			$\phi 4$	-134.8	
			$\psi 4$	35.9	
			$\phi 5$	-154.7	
49	KREAA	1	$\psi 1$	62.5	
			$\phi 2$	-151.6	
			$\psi 2$	49.4	
			$\phi 3$	-93.2	
			$\psi 3$	-49.2	
			$\phi 4$	-140.8	
			$\psi 4$	-49.2	
			$\phi 5$	-127.8	
50	PACAK	1	$\psi 1$	-131.2	
			$\phi 2$	-91.2	
			$\psi 2$	-61.3	
			$\phi 3$	-76.4	
			$\psi 3$	156.4	
			$\phi 4$	-76.5	
			$\psi 4$	156.4	
			$\phi 5$	-97.0	
51	DAICA	1	$\psi 1$	142.1	
			$\phi 2$	-119.1	
			$\psi 2$	-1.3	
			$\phi 3$	-99.7	
			$\psi 3$	44.2	
			$\phi 4$	55.4	
			$\psi 4$	44.2	
			$\phi 5$	-155.1	

52	RAEAD	1	$\psi 1$	119.4.	
			$\phi 2$	-123.1	
			$\psi 2$	5.2	
			$\phi 3$	65.3	
			$\psi 3$	14.6	
			$\phi 4$	-128.0	
			$\psi 4$	14.6	
			$\phi 5$	-139.8	
53	APKKA	1	$\psi 1$	134.5	
			$\phi 2$	-69.4	
			$\psi 2$	-55.5	
			$\phi 3$	-69.8	
			$\psi 3$	-78.3	
			$\phi 4$	-100.0	
			$\psi 4$	-78.3	
			$\phi 5$	-96.6	
54	EAGKA	1	$\psi 1$	115.7	
			$\phi 2$	-128.5	
			$\psi 2$	74.1	
			$\phi 3$	98.2	
			$\psi 3$	117.0	
			$\phi 4$	-137.0	
			$\psi 4$	117.0	
			$\phi 5$	-120.7	

**Supplementary Table 3.** The root-mean-square deviation (RMSD) between the three N- or C-terminal C-alpha atoms of rigid pentapeptides and C-alpha atoms of idealized elements of the secondary structure. The smaller the RMSD value, the higher the similarity of the fragment of the rigid pentapeptide to the idealized secondary structure.

Cluster number	RMSD between N-end of pentapeptide and $\alpha$ -helix	RMSD between N-end of pentapeptide and $\uparrow\downarrow\beta$ -structure	RMSD between N-end of pentapeptide and $\uparrow\uparrow\beta$ -structure	RMSD between C-end of pentapeptide and $\alpha$ -helix	RMSD between C-end of pentapeptide and $\uparrow\downarrow\beta$ -structure	RMSD between C-end of pentapeptide and $\uparrow\uparrow\beta$ -structure
1	0.113	0.573	0.369	0.605	0.136	0.071
2	0.130	0.556	0.352	0.280	0.432	0.227
3	0.150	0.537	0.332	0.081	0.612	0.408
4	0.349	0.339	0.133	0.262	0.449	0.244
5	0.164	0.523	0.318	0.369	0.351	0.146
6	0.298	0.390	0.184	0.813	0.060	0.266
7	0.119	0.567	0.363	0.075	0.617	0.413
8	0.431	0.257	0.051	0.488	0.243	0.038
9	0.040	0.645	0.441	0.422	0.303	0.098
10	0.561	0.125	0.081	0.074	0.618	0.414
11	0.141	0.545	0.340	0.092	0.602	0.398
12	0.001	0.684	0.481	0.028	0.710	0.507
13	0.025	0.709	0.506	0.147	0.553	0.349
14	0.075	0.610	0.406	0.282	0.431	0.226
15	0.226	0.461	0.256	0.192	0.512	0.308
16	0.496	0.191	0.015	0.149	0.551	0.346
17	0.245	0.442	0.236	0.082	0.611	0.407
18	0.130	0.556	0.352	0.404	0.320	0.114
19	0.330	0.357	0.151	0.209	0.497	0.292
20	0.679	0.006	0.201	0.188	0.515	0.311
21	0.312	0.375	0.169	0.496	0.236	0.030
22	0.200	0.487	0.282	0.885	0.128	0.334
23	0.803	0.122	0.328	0.219	0.488	0.283

24	0.402	0.285	0.079	0.459	0.270	0.064
25	0.147	0.539	0.334	0.055	0.635	0.431
26	0.241	0.446	0.241	0.731	0.018	0.188
27	0.153	0.834	0.632	0.077	0.616	0.412
28	0.005	0.689	0.486	0.163	0.538	0.334
29	0.175	0.511	0.306	0.337	0.381	0.176
30	0.647	0.038	0.168	0.458	0.271	0.065
31	0.085	0.600	0.396	0.602	0.138	0.068
32	0.290	0.398	0.192	0.530	0.204	0.002
33	0.754	0.071	0.277	0.411	0.314	0.108
34	0.116	0.570	0.366	0.108	0.588	0.384
35	0.105	0.580	0.376	0.030	0.658	0.454
36	0.035	0.650	0.446	0.427	0.299	0.093
37	0.134	0.552	0.347	0.019	0.667	0.464
38	0.042	0.643	0.439	0.104	0.592	0.388
39	0.513	0.174	0.0327	0.072	0.620	0.417
40	0.334	0.354	0.148	0.038	0.651	0.447
41	0.041	0.644	0.440	0.470	0.259	0.053
42	0.501	0.186	0.0204	0.181	0.522	0.317
43	0.207	0.479	0.274	0.227	0.480	0.276
44	0.057	0.628	0.424	0.611	0.130	0.076
45	0.132	0.554	0.349	0.185	0.518	0.314
46	0.067	0.618	0.414	0.684	0.062	0.145
47	0.868	0.190	0.395	0.215	0.492	0.287
48	0.027	0.658	0.454	0.175	0.528	0.323
49	0.260	0.426	0.221	0.346	0.373	0.168
50	0.216	0.471	0.266	0.571	0.166	0.040
51	0.080	0.605	0.401	0.060	0.738	0.535
52	0.088	0.597	0.393	0.115	0.581	0.377
53	0.079	0.606	0.402	0.3920	0.331	0.125
54	0.278	0.409	0.204	0.610	0.131	0.075